

RESEARCH ARTICLE

Open Access



Genome binding properties of Zic transcription factors underlie their changing functions during neuronal maturation

Melyssa S. Minto^{1,2}, Jesús Emiliano Sotelo-Fonseca³, Vijyendra Ramesh³ and Anne E. West^{3*} 

Abstract

Background The Zic family of transcription factors (TFs) promote both proliferation and maturation of cerebellar granule neurons (CGNs), raising the question of how a single, constitutively expressed TF family can support distinct developmental processes. Here we use an integrative experimental and bioinformatic approach to discover the regulatory relationship between Zic TF binding and changing programs of gene transcription during postnatal CGN differentiation.

Results We first established a bioinformatic pipeline to integrate Zic ChIP-seq data from the developing mouse cerebellum with other genomic datasets from the same tissue. In newborn CGNs, Zic TF binding predominates at active enhancers that are co-bound by developmentally regulated TFs including Atoh1, whereas in mature CGNs, Zic TF binding consolidates toward promoters where it co-localizes with activity-regulated TFs. We then performed CUT&RUN-seq in differentiating CGNs to define both the time course of developmental shifts in Zic TF binding and their relationship to gene expression. Mapping Zic TF binding sites to genes using chromatin looping, we identified the set of Zic target genes that have altered expression in RNA-seq from Zic1 or Zic2 knockdown CGNs.

Conclusions Our data show that Zic TFs are required for both induction and repression of distinct, developmentally regulated target genes through a mechanism that is largely independent of changes in Zic TF binding. We suggest that the differential collaboration of Zic TFs with other TF families underlies the shift in their biological functions across CGN development.

Keywords Zic transcription factors, Cerebellar granule neuron maturation, Genome binding dynamics, Bioinformatic analyses, Developmental gene expression, Transcription factor collaboration

Background

The dynamic expression and function of transcription factors (TFs) underlie the changing programs of gene expression that define stages of cellular differentiation during development [1, 2]. TFs orchestrate cellular differentiation by binding in a sequence-specific manner to accessible gene regulatory elements. TFs also cooperate with co-activator and co-repressor complexes to influence the state and structure of chromatin. Thus, the regulatory function of any given TF is determined not only by when and where it is expressed but also by a confluence of factors that determine where and how that TF

*Correspondence:

Anne E. West
west@neuro.duke.edu

¹ Program in Computational Biology and Bioinformatics, Duke University, Durham, NC 27710, USA

² Omics, Epidemiology and Analytics Program, RTI International, Research Triangle Park, NC 27709, USA

³ Department of Neurobiology, Duke University, Durham, NC 27710, USA



© The Author(s) 2024. **Open Access** This article is licensed under a Creative Commons Attribution-NonCommercial-NoDerivatives 4.0 International License, which permits any non-commercial use, sharing, distribution and reproduction in any medium or format, as long as you give appropriate credit to the original author(s) and the source, provide a link to the Creative Commons licence, and indicate if you modified the licensed material. You do not have permission under this licence to share adapted material derived from this article or parts of it. The images or other third party material in this article are included in the article's Creative Commons licence, unless indicated otherwise in a credit line to the material. If material is not included in the article's Creative Commons licence and your intended use is not permitted by statutory regulation or exceeds the permitted use, you will need to obtain permission directly from the copyright holder. To view a copy of this licence, visit <http://creativecommons.org/licenses/by-nc-nd/4.0/>.

is recruited to the genome [3, 4]. Our understanding of the regulatory logic of TF binding has been advanced in recent years by analysis of genome-wide sequence studies that describe the chromatin and TF landscape in a wide range of different cell types and cell states [5].

Members of the zinc fingers of the cerebellum (*Zic*) family (*Zic1*–*Zic5*) of C2H2 zinc finger TFs are broadly expressed in dorsal neuronal progenitors during vertebrate embryogenesis [6]. The *Zics* function to delay the exit of neural progenitors from the cell cycle, which ultimately results in the production of more neurons and larger brains [7, 8]. The *Zics* also function in neuroblasts to promote migration, both in the embryonic brain and in the subventricular zone and rostral migratory stream of the adult rodent brain [9, 10]. Knockout of the *Zic* genes in mice result in significant brain developmental defects including microcephaly, abnormal cerebellar patterning, and dysgenesis of medial structures [11]. These neural progenitor phenotypes are similar to the effects of *Zic* loss-of-function mutations in human disorders, including cerebellar hypoplasia associated with *ZIC1* and *ZIC4* mutations in Dandy-Walker Syndrome [12] and *ZIC2* mutations in holoprosencephaly [13].

Despite their established functions as drivers of neuronal progenitor proliferation, the *Zic* TFs remain expressed into adulthood in select populations of differentiated neurons, including GABAergic interneurons of the olfactory bulb [10] and striatum [14], thalamic neurons [15], and most notably granule neurons of the cerebellum (CGNs) [16]. Because *Zic* knockout mice have early developmental phenotypes, little is known about the specific functions of the *Zic* TFs in differentiated neurons or how they stop promoting cellular proliferation as neurons mature.

The development of CGNs in the postnatal mouse cerebellum is a useful model system to discover the mechanisms of chromatin regulation that orchestrate postmitotic stages of neuronal differentiation and maturation [17]. There are temporally coordinated changes in chromatin accessibility and gene transcription that correlate with these developmental stages [18]. Germline knockouts of *Zic1*, *Zic2*, *Zic3*, and *Zic4* in mice are all associated with hypoplastic cerebellum due to reduced

numbers of CGNs demonstrating their requirement in CGN progenitors [6–8]. In addition, *Zic* binding is found in the gene regulatory elements that become more accessible as CGNs mature, indicating that this TF family has functions in differentiated CGNs beyond their roles in progenitors [18]. By ChIP-seq, we observed that *Zic* distribution across the genome changes as CGNs mature, and we speculated that the shift in *Zic* binding could underlie a biological change in *Zic* function. However, the functional consequences of changes in *Zic* TF binding for the regulation of developmental gene expression was unknown.

Here, we first establish a bioinformatic pipeline to integrate *Zic* ChIP-seq data from the developing mouse cerebellum with other genomic datasets from the same tissue and show how genomic location, DNA sequence, and chromatin features of *Zic* TF binding sites correlate with changes in gene expression over development. We then perform CUT&RUN-seq in differentiating CGNs, map *Zic* TF binding sites to genes using chromatin looping data and identify *Zic* target genes that have altered expression in RNA-seq from *Zic1* or *Zic2* knockdown CGNs. These data establish an experimentally validated set of developmentally regulated *Zic* TF target genes and suggest that the collaboration of *Zic* TFs with other TF families defines the changing biological function of *Zic* TFs over the course of CGN differentiation.

Results

Zic TF binding consolidates from distal enhancers to promoters over CGN maturation

To characterize the genomic features of *Zic* binding over the course of CGN maturation, we aligned *Zic* 1/2 ChIP-seq data [18] to the GRCm38 Gencode vM21 genome. This allowed us to compare *Zic* TF binding sites (peaks) to genome features and chromatin state data from other genomic datasets available from this same tissue. Of 56,941 *Zic* peaks, approximately 39% were significantly different between time-points (“dynamic”). 10,468 peaks were enriched at P60 (“late” peaks), and 11,721 peaks were enriched at P7 (“early” peaks). 34,752 *Zic* ChIP peaks were not significantly different between P7 and P60 (“static” peaks) (Fig. 1A, Additional file 2). Because single

(See figure on next page.)

Fig. 1 *Zic*1/2 binding is dynamic across mouse cerebellar development. **A** MA plot comparing *Zic* ChIP-seq peaks at P7 and P60. Red, significantly increased (“Late peaks”); blue, significantly decreased (“Early peaks”) (FDR < 0.05). **B** Distribution of the mean normalized reads in early and late *Zic* ChIP peaks at P7 and P60. **C** Total number of dynamic early and late *Zic* ChIP-seq peaks that were either completely lost as CGNs mature (Early) or newly gained between P7 and P60 (Late) as defined in the results text. **D** Example tracks of peaks that were lost as CGNs mature or gained between P7 and P60. **E** Proportion of *Zic*1 and *Zic*2 motifs found in the dynamic and static *Zic* ChIP peaks. **F** Overlap (black) or nonoverlap (gray) of *Zic* ChIP peaks with H3K27ac peaks, DNase hypersensitive sites (DHS), or both. **G** The distribution of dynamic and static *Zic* ChIP-seq peaks with respect to genomic features

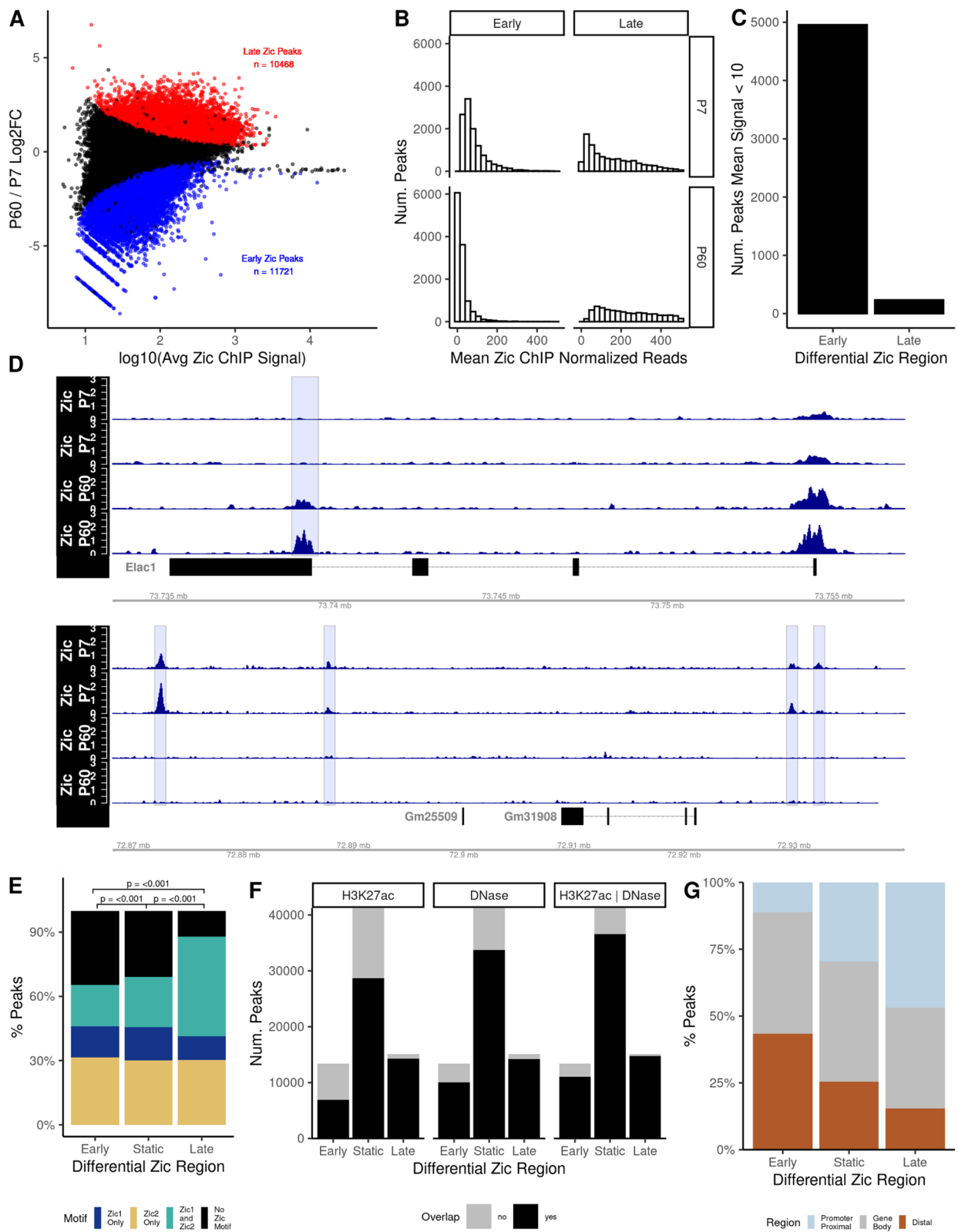


Fig. 1 (See legend on previous page.)

cell sequencing studies show that CGNs comprise ~60% (P7) to >90% (P60) of all cerebellar cells [19], and both *Zic1* and *Zic2* are highly expressed in these cells, we interpret the changes in *Zic* binding profiles we observe by bulk cerebellar ChIP-seq to predominantly arise from CGNs. However, *Zic1* and *Zic2* are also expressed in postnatal astrocytes, which comprise up to 15% of cerebellar cells [19], thus a fraction of our differential *in vivo* ChIP-seq signal could reflect developmental shifts in the CGN to astrocyte ratio.

Dynamic peaks could either reflect binding sites that are fully gained or lost during CGN differentiation, or they could be binding sites where the magnitude of *Zic* TF binding increases or decreases over time. To resolve these possibilities, we defined early and late peaks with an average read count of <10 at the other time point as those exhibiting complete loss or gain. We observed that very few (~400) late *Zic* peaks had <10 normalized average reads at P7, whereas there was a much higher number of early *Zic* peaks (~6000) with low average reads at P60 (Fig. 1B, C). Overall, 42.7% of the early peaks are lost as CGNs mature, whereas only 3.8% of the late peaks are newly gained (Fig. 1D). These data show that *Zic* binding consolidates over time such that there is more binding at a smaller number of sites as CGNs mature.

The average width of *Zic* ChIP peaks is 528 bp (Additional file 1: Fig. S1A), which could allow for binding of multiple *Zic* TFs within a single peak. To assess the composition of *Zic* binding sites within the *Zic* ChIP peaks, we searched for *Zic* motifs in early versus late peaks. We calculated the percentage of *Zic* ChIP peaks that contained either *Zic1* motifs (Additional file 1: Fig. S1B) or *Zic2* motifs (Additional file 1: Fig. S1C) using the FIMO tool from the MEME suite [20, 21]. Most peaks had only a few (0–4) *Zic1* or *Zic2* motifs even though the fragments were large (Additional file 1: Fig. S1D). Among the early and static peaks, the *Zic2* motif was the most common, with a smaller proportion of peaks containing the *Zic1* motif. Over 25% of peaks contained neither motif, suggesting that *Zic* might bind these sites in a non-canonical way either through targeting different sequences or via indirect binding. In contrast, the late sites were more highly enriched for peaks with both *Zic1* and *Zic2* motifs (Fig. 1E, Additional file 1: Fig. S1D). This supports the idea that *Zic* binding is consolidating at the late timepoint with the increase in both motifs and greater likelihood of direct *Zic* binding.

The *Zic* TFs are traditionally known as transcriptional activators, though in some contexts they can function in gene repression [22]. Histone modifications reflect the activation state of cis-regulatory elements, with histone H3 lysine 27 acetylation (H3K27ac) serving as a marker of active enhancers and promoters. To determine whether

Zic TFs are associated with active regulatory elements during early and late stages of CGN differentiation, we examined the overlap of *Zic* peaks with accessible and active regions of chromatin, as determined by DNase hypersensitivity (DHS) and ChIP-seq for H3K27ac at P7 and P60 [18]. Early, late, and static *Zic* binding were all largely within regions of active chromatin indicated by overlap with DHS sites and/or H3K27ac ChIP-seq regions (Fig. 1F). These data demonstrate that the *Zic* TFs are predominantly binding to open and active chromatin.

Genome-wide binding profile studies have revealed that TFs can act either by binding proximal promoters or by binding to distal enhancers, with some TFs showing a preference for one or the other location [23]. *Zic* ChIP-seq peaks were annotated by location in the genome with respect to nearest transcription start sites, and these data showed that the distribution of *Zic* binding significantly shifts across CGN maturation. The early *Zic* peaks are nearly evenly split between gene bodies and distal enhancers, with fewer sites in proximal promoters. The late peaks are shifted in distribution toward proximal promoters, which comprise nearly 50% of all *Zic* peaks in the late peaks (Fig. 1G). The static sites showed an intermediate distribution. Taken together, these data suggest that the binding of the *Zic* TFs consolidate from a large set of distal enhancers to a more focused set of gene promoters in maturing neurons.

Distinct families of TFs are associated with early versus late *Zic* TF ChIP-seq peaks

The *Zic* TFs are known to cooperate with other TFs either directly through protein–protein interactions or indirectly through co-regulation of target genes [22]. We reasoned that bioinformatic analysis of the *Zic* ChIP-seq peaks might reveal TFs that collaborate with the *Zic* TFs to regulate target genes. To identify these putative *Zic* TF co-regulators, we made the assumptions that TFs working with *Zic* TFs differentially over time would (1) bind close to *Zic*, within the regions defined as *Zic* ChIP-seq peaks, and (2) may be differentially expressed during stages of CGN development.

We interrogated the sequence of the *Zic* ChIP-seq peaks to identify enriched TF binding motifs using the motif discovery program HOMER (FDR < 0.05, $n = 205$) [24]. In parallel, we assessed the genomic locations of the early and late *Zic* ChIP-seq peaks for overlap with published ChIP-seq binding data for TFs using the Binding Analysis for Regulation of Transcription (BART) tool (FDR < 0.05, $n = 326$) [25]. The combination of these methods allowed us to consider both direct and indirect genomic association of other TFs with the *Zics* as a possible mechanism for co-regulation of these regions (Additional file 3). The HOMER and BART tools each

contain data on a large and overlapping set of TFs (Additional file 1: Fig. S2A–C). Many of the enriched TFs were shared between the early and late sites (Additional file 1: Fig. S2A–B). To discover TFs that may distinguish Zic function between developmental stages, we used a Rank-Rank Hypergeometric overlap (RRHO) test to find the TFs whose enrichment *p*-values were discordant between early and late Zic-ChIP peaks (Additional file 1: Fig. S2D–E). Out of 205 enriched motifs, 35 are distinctly enriched in the early Zic peaks, and 34 are distinctly enriched in the late Zic peaks set (Fig. 2A). Out of the 326 TFs whose ChIP binding was enriched in the early or late peak sets from BART, 53 were distinctly enriched early, and 29 were distinctly enriched late (Fig. 2B). Distinctly enriched TFs were then filtered for concordant temporal transcriptional enrichment using the RNA-seq data [18] resulting in 65 predicted co-regulators of Zic in early CGN maturation and 23 predicted co-regulators of Zic in late CGN maturation (Fig. 2C, D).

Workflow captures both known and novel putative Zic co-regulatory TFs

Consistent with prior evidence that the Zic TFs collaborate with other developmental TFs in neural progenitors [11], early Zic sites were enriched for Homeobox and bHLH domain -containing TFs. Most notably, the bHLH TF *Atoh1*, which is a fate-determining factor for differentiation of CGN progenitors, was identified by BART as strongly enriched in the set of early Zic ChIP-seq peaks (Fig. 2D). In the mouse cerebellum, *Atoh1* is highly expressed in granule neuron progenitors from E12.5 to P14, where it binds directly to DNA sequences that contain a specialized E-Box-like motif [26–30]. *Atoh1* expression is downregulated after progenitors leave the cell cycle, and it is not expressed in postmitotic CGNs [30]. To quantify the overlap of *Atoh1* binding with the Zic TFs, we obtained a dataset of *Atoh1* ChIP-seq from P5 mouse cerebellum [26] and examined the overlap of *Atoh1* binding sites with our static and dynamic Zic ChIP-seq peaks (Additional file 3). These data revealed

that 54.7% *Atoh1* peaks overlap the full set of Zic ChIP-seq peaks (Fig. 2E). Importantly, as we predicted, *Atoh1* ChIP peaks overlap a greater percentage of the early Zic peaks compared with static and late Zic peak (*chi-sq* *p*-value < 0.05) (Fig. 2F). These data showed evidence for convergent Zic/*Atoh1* regulation of genes known to be important in CGN development like the chromatin regulator *Chd7* [31] (Fig. 2G). Among the other early expressed TFs that were associated with early Zic sites were several known to be involved in cell proliferation via Wnt, FGF, Notch, and SMAD signaling pathways (Fig. 2A–D). These factors include *Tfap4* [32, 33], RFX proteins [34], and TCF proteins [35], which are co-effectors in Wnt/ β -catenin pathways, and SMAD proteins, which are activators of TGF-beta signaling and downstream of BMP signaling [36–38]. Early Zic sites are also co-localized with binding of TFs that have established functions in axon guidance (*Nkx2.2*) [39] and enriched for motifs of TFs that function in cellular migration (*Pbx3*, *Pknox1*, *Lhx1*), deepening understanding of how Zic TFs may promote CGN proliferation and migration.

Using the BART dataset in our workflow allowed us to query our Zic binding cis-regulatory regions in prior ChIP-seq datasets to predict potential Zic co-regulatory chromatin factors, because these factors do not bind directly to DNA. Proteins that are members of or interact with cohesin complex (CTCF, RAD21, SMCHD1, SMC3, STAG1, AND TOP2B) [40], Polycomb complexes (BMI1, PCGF2, PCGF6, PHC1, PHF19) [41], HP1 complex (CBX5, TRIM28) [42, 43], NuRD Complex (MBD3, TRIM28) [44, 45], REST complex (RCOR2, REST) [46], and BAF complex (ARID3A, BCL11A, SMARCA1, TOP2B) [47] were all enriched in the early versus late Zic binding sites (Fig. 2A, C). We noticed that many of these are transcriptional repressor complexes or factors involved indirectly in gene regulation via chromatin architecture. These data suggest that functions of the Zic TFs extend beyond direct activation of target genes.

In contrast to our analysis of the early Zic TF peaks, we found very few hits in BART that colocalized with the

(See figure on next page.)

Fig. 2 Distinct TF binding sites are enriched in early and late Zic ChIP peaks. Motif enrichment analysis using HOMER and ChIP-seq peak overlap enrichment analysis using BART was performed on the set of early and late Zic ChIP peaks to find potential collaborators of Zic TF binding. A rank-rank hyper-geometric overlap test was performed to identify the distinctly enriched **A** motifs and **B** TF ChIP-seq profiles between early and late Zic peaks where blue points are TF binding enriched in early Zic peaks and brown points are TF binding enriched in late Zic peaks. This set of time-point specific enriched TF **C** motifs and **D** TF ChIP-seq profiles within early and late Zic peaks were filtered for transcriptional enrichment at the respective time-points (P7 or P60). Each point is colored and sorted by the TF enrichment adjusted *p*-value, and the size of each point is the average expression of the mapped gene in RNA-seq data at the respective time point. Log₂ FC (fold change). **E** The proportion of ChIP-seq peaks that are co-occupied by Zic peaks colored by the enrichment of the Zic peak (red—enriched at P60, blue—enriched at P7, black—static, and gray—no Zic peak) and **F** the proportion of overlap (gray) or nonoverlap (black) of *Atoh1* ChIP-seq peaks that overlap Zic peaks separated by “early” (P7 enriched), static, and “late” (P60 enriched) peaks for *Atoh1* in cerebellum at P5 [26]. **G** Example tracks for *Chd7* at P5 overlapping with Zic binding (gray bars) in P7 or P60 cerebellum

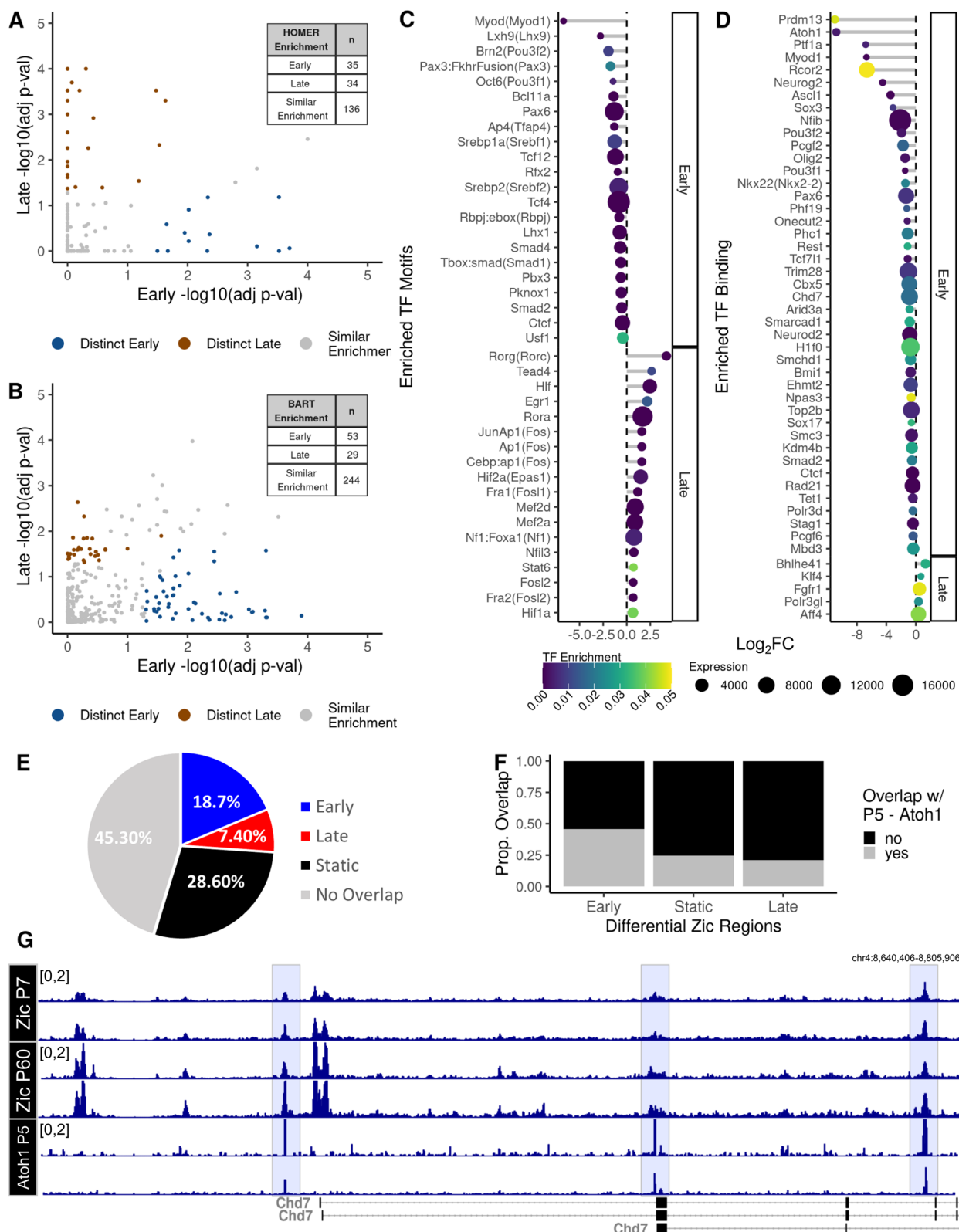


Fig. 2 (See legend on previous page.)

late Zic TF peaks (Fig. 2D). This is likely a limitation of the database, which predominantly contains ChIP-seq data from dividing cells rather than postmitotic neurons. However, we did find enrichment in the late Zic TF peaks using HOMER of motifs for several TFs that show elevated expression in maturing CGNs. These include RORa and RORc, two factors involved in retinoid acid induced neuronal differentiation [48] (Fig. 2C), as well as Hif1a which plays an important role in oxygen-dependent CGN cell-cycle exit [49] (Fig. 2D). Most strikingly, the HOMER results suggest a role for activity-dependent transcription TFs as potential Zic TF collaborators. In the late Zic peaks, we see enrichment for binding sites of canonical activity-regulated TFs including FOSL2, FOS, JUN, EGR1, MEF2A, and MEF2D (Fig. 2C). At the genomic level, AP-1 transcription factors of the FOS and JUN families have been shown to promote chromatin accessibility, which can help developmentally regulated TFs to bind and could facilitate Zic binding at the late peaks we detect in mature CGNs [50]. At a functional level, activity-regulated TFs, especially those of the MEF2 family, are important in regulating synaptic refinement, which is a key late developmental process in postmitotic neurons [51, 52].

Determining Zic TF regulatory activity by chromatin looping

Up to this point, we have analyzed features of Zic binding with respect to their local sequence and chromatin features, but we have not yet considered the relationship between Zic TF binding and the transcriptional regulation of genes. As we show in Fig. 1G, at most ~50% of Zic ChIP-seq peaks are in proximal promoters, where they can be likely to regulate the nearest gene. TFs bound far away in linear space from their target genes are thought to come into close three-dimensional proximity with their target gene promoters via structural looping [53]. Thus, to identify the likely target genes of the Zic TFs, and to advance understanding of the relationship between developmentally regulated Zic binding and differential gene expression, we integrated our Zic ChIP-seq data with two different datasets of chromatin conformation [54–56] from the developing mouse cerebellum. One

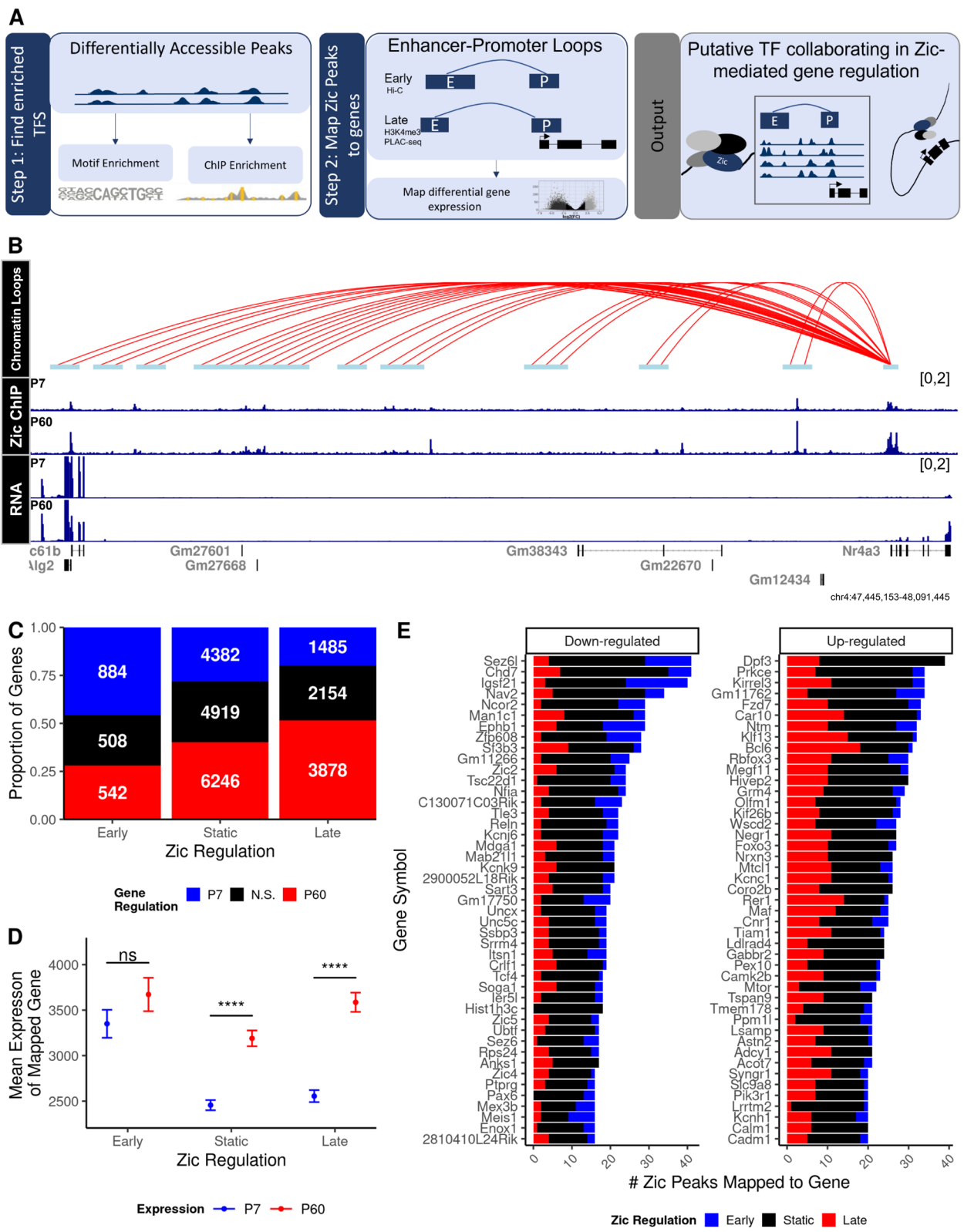
study used antibodies against H3K4me3 to perform promoter-centered Proximity Ligation-Assisted ChIP-seq (PLAC-seq) from adult (P56) mouse cerebellum [54] and the other used Hi-C to identify chromatin loops in cerebellum from juvenile (P22) mice [55, 56]. We validated that Zic ChIP peaks colocalize with anchors from both datasets and that the late Zic peaks preferentially overlap the anchors from P56 as we would expect (Additional file 1: Fig. 3, Fig. S3A, B). However, because the anchors identified in each dataset are largely non-overlapping (Additional file 1: Fig. S3, Fig. 3C), we filtered early, late, and static Zic peaks for those that were within anchors of the captured chromatin loops in either dataset and used this union set for comparison to expression of the associated gene (Fig. 3A). For example, the *Nr4a3* gene, whose expression increases at P60, has promoter-enhancer loops more than 600 Kb upstream containing Zic peaks (Fig. 3B). Using this approach, the intersecting Zic peaks in enhancers can be mapped to the promoters of genes they may regulate (Additional file 4). Indeed, a higher proportion of genes linked to anchors that have early Zic peaks are significantly more highly expressed at P7 and vice versa for late peaks and expression at P60 (Fig. 3C). These data show that we can use chromatin conformation data to predict developmental relationships of distal Zic binding sites with gene expression.

To determine the relationship between Zic binding and gene transcription, we first assessed the average expression level at P7 and P60 of genes that map to early, static, or late Zic peaks. Overall, the expression of all the genes mapped to Zic peak-overlapping anchors rose at P60, with genes mapped to the static and late peaks showing significant increases (Fig. 3D). Notably, the genes mapping to early Zic binding sites did not show a decrease in gene expression over time. This suggests that the loss of Zic is not a driving factor for transcriptional downregulation in maturing CGNs. However, these data do suggest that Zic has a transcriptional activating role in late stages of CGN maturation.

We next asked if the number of Zic binding events was a proxy for regulatory activity by determining if expression at any given time point or fold change in expression from P7 to P60 was a function of the number of Zic

(See figure on next page.)

Fig. 3 Zic binding sites can be mapped to genes through chromatin looping. Zic ChIP peaks were overlapped with anchors derived from cerebellar Hi-C [56] and H3K4me3 PLAC-seq [54] data. **A** Schematic of peak mapping workflow using chromatin looping data. **B** Example tracks of H3K4me3 loops interacting with the *Nr4a3* gene 100 MB upstream, Zic ChIP-seq at P7 and P60, and RNA-seq at P7 and P60. **C** Overall number of genes mapped to early, static, and late Zic ChIP-seq peaks. **D** Expression of genes at P7 and P60 mapped to early, static, and late Zic ChIP-seq peaks. Graph shows mean and standard deviation of gene expression. *** denotes a significant difference in the mean expression between P7 and P60 with a Bonferroni adjusted $p < 2.2e-6$ using a pairwise *t*-test. **E** Top 50 downregulated (FDR < 0.0f, LFC < 0) and upregulated (FDR < 0.05, LFC > 0) genes by the number of mapped Zic ChIP-seq peaks that are dynamic between P7 and P60. Red indicates ChIP-seq peaks enriched at P60 (late), blue indicates enriched at P7 (early), and black indicates static peaks



peaks that mapped to a gene. We calculated the number of early, static, and late Zic peaks that could be mapped to each gene (Fig. 3E, Additional file 1: Fig. S4A, B). We found a weak correlation between the number of Zic peaks and average expression ($\rho=0.2$, $p < 2.2e-16$) and degree of fold change ($\rho=0.11$, $p=1.3e-14$) (Additional file 1: Fig. S4C, D). When we looked at the top 30 genes with the most mapped Zic peaks, we saw qualitative evidence that developmentally downregulated genes were more likely to have Zic sites that were eliminated by P60 and that developmentally induced genes were most likely to gain Zic sites (Fig. 3E); however, substantial Zic TF binding was static for both sets of genes. Taken in isolation, the number of Zic binding sites has a detectable but weak monotonic association with gene expression.

Identification of genes that require Zic1/2 for their developmental expression

Taking chromatin looping into account helped us focus on genes that could be direct transcriptional targets of the Zic TFs. However, it is clear from our data that binding of Zic alone is not sufficient to identify genes that require Zic for their transcription; thus, incorporation of a functional molecular genomic analysis is required. In a prior study, we knocked down (KD) expression of Zic1 or Zic2 in CGNs differentiating in culture and characterized changes in gene expression [18]. Thus, here, to validate direct targets of Zic TF regulation in CGNs, we first conducted CUT&RUN-seq to map static and dynamic sites of Zic1/2 binding sites across the genome of CGNs after 1,3,5 and 7 days of differentiation in vitro (DIV). We then integrated these data with chromatin looping as well as RNA-seq showing dynamic changes in gene expression over this course of development in control and Zic KD neurons (Additional file 5).

Our CUT&RUN-seq data allowed us to refine the time course of Zic TF binding dynamics during CGN differentiation. Comparing called Zic TF peaks at DIV7 vs. DIV1 revealed 3919 downregulated peaks and 2832 upregulated peaks ($FDR < 0.05$), demonstrating our

ability to capture dynamic Zic binding in this culture system (Additional file 1: Fig. S5A-F). Of the sequential comparisons, DIV3 vs. DIV1 had the greatest number of significant changes (UP=1544, DOWN=746) compared to DIV5 vs. DIV3 (UP=13, DOWN=299) and DIV5 vs. DIV7 (UP=70, DOWN=51). To determine how changes in Zic TF binding during differentiation in culture relate to the dynamics over the timeframe we analyzed in vivo, we performed a principal component analysis (PCA) of the Zic ChIP-seq and the Zic CUT&RUN peaks to cluster the samples (Additional file 1: Fig. S5G, H). PC1 separates the samples by developmental time, and when we considered all the samples together, the culture time points all cluster very closely together compared with the P7 to P60 separation. Along PC2, DIV1 peaks are closer to the in vivo P7 peaks and DIV7 peaks are closer to in vivo P60 peaks (Fig. 4A). Early in vivo Zic ChIP-seq peaks preferentially overlapped DIV3 Zic CUT&RUN peaks and late in vivo Zic ChIP-seq peaks preferentially overlapped DIV7 CUT&RUN peaks (Fig. 4B). DIV3 peaks have more overlap with early in vivo peaks (58%) than late in vivo peaks (2%), while DIV7 peaks have more overlap with late in vivo peaks (33%) than early in vivo peaks (3%) (Fig. 4B). These data indicate that our culture results are enriched for the Zic TF binding events that happen at very early stages of CGN differentiation in vivo; however, they also support our ability to use the culture system to compare changes in Zic TF genomic binding to concordant changes in target gene transcription. Importantly, because the cellular composition of our cultures does not change, the gradual and continuous changes we observe in the intensity of Zic CUT&RUN peaks across all four time points (Additional file 1: Fig. S5I) further supports our hypothesis that Zic TFs are developmentally redistributed across the genome as CGNs mature.

We focused our analysis on the DIV3 and DIV7 Zic CUT&RUN peaks because these time points align with our previous Zic KD RNA-seq [18]. Differential analysis of the 49,296 Zic CUT&RUN peaks in the merged dataset revealed 1543 peaks enriched at DIV7, 3049 peaks

(See figure on next page.)

Fig. 4 Identification of developmentally regulated and Zic-dependent genes in CGNs differentiating in culture. **A** Principal component analysis of Zic binding data in culture and in vivo using the SEACR-called CUT&RUN peaks of in culture and in vivo samples. **B** Overlap of in vivo Zic ChIP-seq Early and Late peaks with Zic CUT&RUN peaks enriched 3 days in vitro (DIV3) versus 7 days in vitro (DIV7). **C** MA plot of Zic CUT&RUN peaks called by SEACR at DIV3 versus DIV7. **D** Example of differential peak within *Ebf3* between DIV3 and DIV7. **E** Distribution of the size (widths) of Zic CUT&RUN peaks in a union set of the data from DIV3 and DIV7. **F** The genomic distribution of Zic binding sites in DIV3-enriched, static, and DIV7-enriched Zic CUT&RUN peaks. **G** Fold change of differentially regulated genes comparing DIV7/DIV3 (developmental, left) and Zic1 KD (top) or Zic 2 KD (bottom) versus shRNA control at DIV7. Genes in the left most panels are developmentally regulated genes but unaffected by Zic KD, the genes in the middle panels are significantly upregulated or downregulated by Zic KD but their expression do not change from DIV3 to DIV7, and the genes in the right panels are Zic-dependent developmentally regulated genes. The colors represent whether the expression of the gene was dependent on Zic1 (dark blue), Zic2 (yellow), or both (light blue) and the size of the point represents the number of DIV3 and DIV7 union set Zic1/2 CUT&RUN peaks mapped to the gene

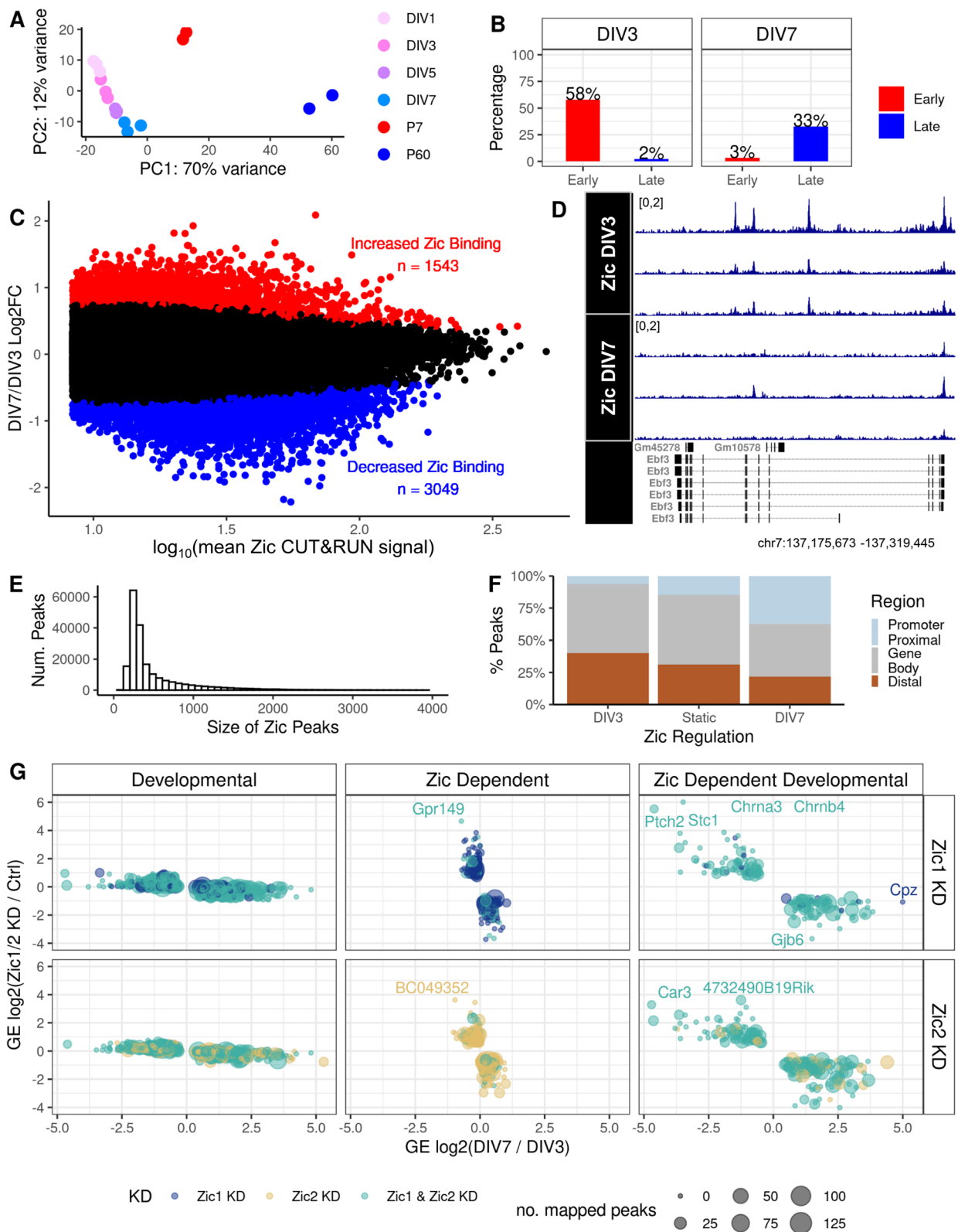


Fig. 4 (See legend on previous page.)

enriched at DIV3, and 44,704 static Zic peaks (Fig. 4C; Additional file 5). One example of Zic binding loss in vitro is at the developmentally downregulated *Ebf3* gene (Fig. 4D). Like the P7/P60 Zic ChIP-seq peaks, the DIV3/DIV7 Zic CUT&RUN peaks sizes are large enough to allow for binding of multiple TFs, with a median size of 317 bp (Fig. 4E). Additionally, the Zic CUT&RUN peaks show a similar shift from overlapping distal enhancers to consolidating at promoter proximal regions as CGNs mature (Fig. 4F). Thus, our CGN culture system recapitulates key aspects of in vivo developmental Zic binding dynamics.

We used DIV3, DIV7, and Zic1/2 KD RNA-seq data [18] to identify developmentally genes that are also regulated by Zic1 and/or Zic2. Comparing DIV3 to DIV7 revealed 1388 upregulated and 855 downregulated developmental genes (Additional file 1: Fig. S6A); comparing Zic1 KD vs. control shRNA at DIV7 showed 277 upregulated and 264 downregulated Zic1-dependent genes (Additional file 1: Fig. S6B); and comparing Zic2 KD vs. control shRNA at DIV7 revealed 303 upregulated and 435 downregulated Zic2-dependent genes (Additional file 1: Fig. S6C). Finally, to identify the set of Zic-dependent developmental genes (ZDDs), we performed pairwise RRHO analyses to find the genes that showed a discordant expression upon Zic1 or Zic2 KD (Additional file 1: Fig. S6D, E). This analysis yielded genes in three categories: (1) developmentally regulated but Zic-independent ($n=1582$), (2) Zic1- or Zic2-dependent but not developmentally regulated ($n=455$), and (3) Zic1- or Zic2-dependent and developmentally regulated (ZDDs, $n=329$) (Fig. 4G; Additional file 5).

We used the ZDD genes to determine how Zic binding relates to changes in gene expression. To identify direct Zic targets from the ZDD gene list, we asked which of these genes had Zic TF CUT&RUN peaks associated with their promoters via chromatin loops following the workflow described in Fig. 3A. Thirty-seven ZDD genes had anchors that overlapped Zic CUT&RUN peaks. Notably, this analysis identified direct Zic target genes that required Zic for repression as well as genes that required Zic for induction over developmental time,

which we discuss further below. If changes in Zic TF binding were driving the developmental regulation of these genes, we would predict that Zic binding events at these anchors would be dynamically regulated between DIV3 and DIV7. However, the Zic CUT&RUN peaks that mapped to the ZDD genes were mostly static between DIV3 and DIV7 (Fig. 5A). For example, *Ets2* is a gene that fails to upregulate over time in culture when Zic1/2 are knocked down, yet most of the Zic TF binding at the *Ets2* promoter and associated enhancers is static between DIV3 and DIV7 (Fig. 5B). Thus, similar to our analysis of differential Zic binding in vivo, we conclude that developmental changes in Zic binding are not required for changes in target gene expression.

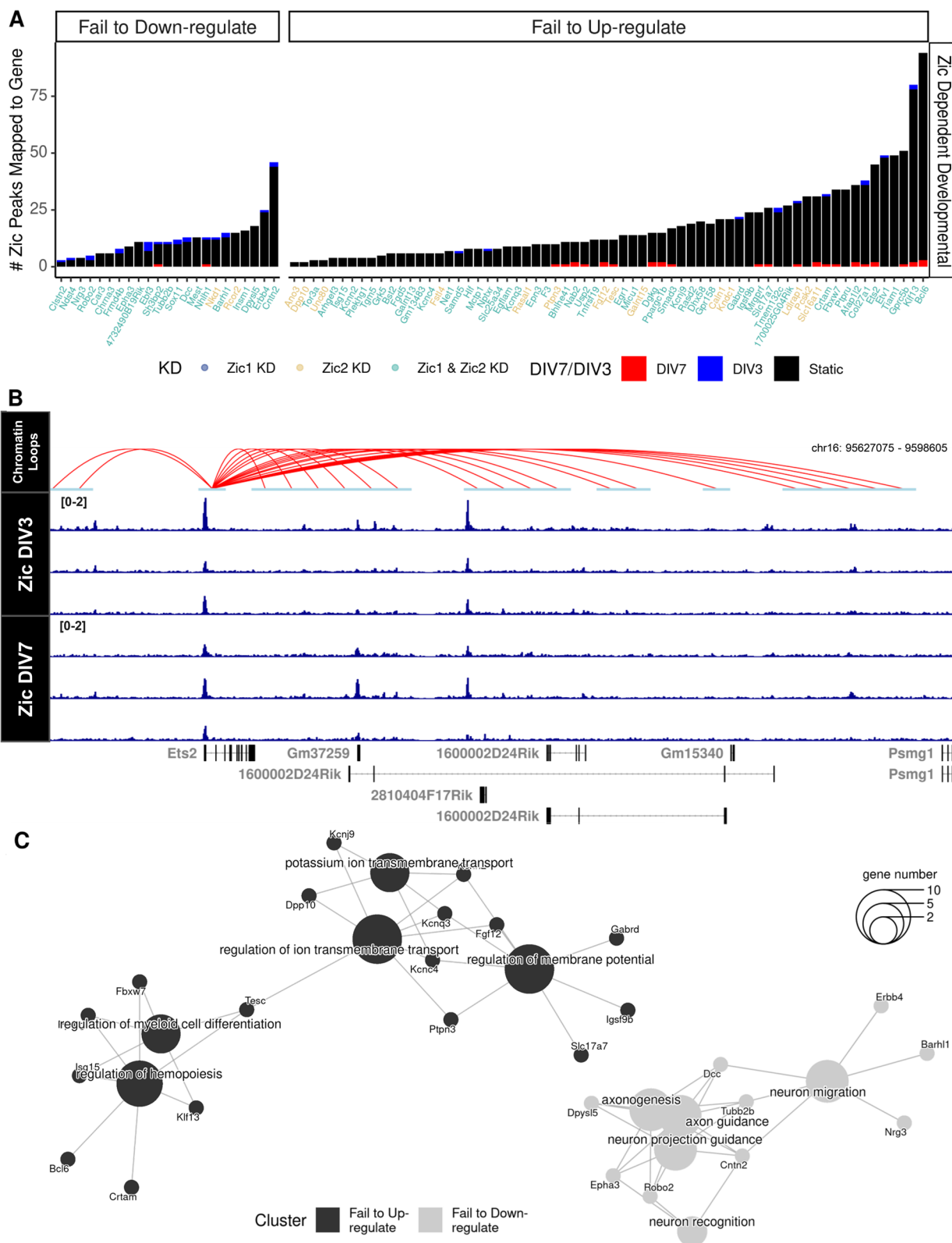
Finally, because the ZDD genes are validated direct targets of transcriptional regulation by the Zic TFs, they offer insight into the function of these TFs during CGN differentiation and maturation. To understand the functions of these Zic targets, we performed GO enrichment analysis on the Biological Processes (BP) terms for the ZDD genes (Fig. 5C; Additional file 5). Zic TF target genes that were downregulated between DIV3 and DIV7 were enriched for GO BP terms including “neuron migration” and “axonogenesis” that define early stages of brain development and neuronal morphogenesis including *Dppyl5* [57], *Dcc* [58], and *Tubb2b* [59]. By contrast, Zic TF target genes that were upregulated between DIV3 to DIV7 were enriched for GO BP terms including “regulation of ion transport channels” and “regulation of membrane potential” that relate to aspects of neuronal function. These genes encode several synaptic receptor and ion channels including the pyruvate transporter *Slc16a11*, the GABA receptor subunit *Gabrd*, and members of the *Kcn* potassium channel and *Ptp* protein tyrosine phosphatase gene families.

Discussion

We implemented an integrative experimental and bioinformatic approach to understand how Zic family TFs change their function over the course of CGN differentiation. By interrogating the underlying sequence and genomic context of Zic ChIP-seq peaks in early and late

(See figure on next page.)

Fig. 5 Candidate direct targets of Zic TF repression and activation converge on processes that underlie neuronal maturation. **A** Zic CUT&RUN peaks were mapped to each Zic-dependent developmental gene. Colors of the bar indicate the timepoint in which peaks are enriched (Blue, DIV3 enriched, red, DIV7 enriched, black, static) and colors of the genes indicate whether the expression of the gene was dependent on Zic1 (dark blue), Zic2 (yellow), or both (light blue). Genes are separated by their developmental up- or downregulation between DIV3 to DIV7 in CGN cultures. **B** Example track of static Zic TF binding with chromatin loops from cultured CGNs near a Zic-dependent gene that fails to upregulate upon Zic KD (*Ets2*). **C** Cluster diagram of biological process gene ontologies for genes that failed to be upregulated (black) and genes that failed to be downregulated (gray) in the Zic1 or Zic2 knockdown. The size of the center circle indicates the number of genes in each of the categories shown. The smaller circles show specific ZDD genes, and the lines connect those genes to their biological process category. Some genes are linked to more than one biological process



stages of CGN maturation, we identified developmental stage-specific features of Zic TF binding sites and determined the relationship of Zic TF binding dynamics to effects on transcription. Our results suggest that the Zic TFs both activate and repress transcription to promote maturation of postmitotic CGNs. The Zic ChIP-seq data support a model whereby Zic TFs bind widely to distal enhancers in early development to support chromatin organization and then consolidate at promoter regions in maturing CGNs to facilitate the expression of genes involved in neuronal maturation. However, Zic-dependent changes in developmental gene expression can occur even in the absence of changes in Zic TF binding, and we suggest that other TF families collaborate with Zic to define the regulatory logic of Zic TF function in neuronal maturation.

The Zic TFs are known to collaborate with other TFs in early development to regulate transcription in many cell types [22]. For example, Zic1 has been shown to form a complex with Pax3 and Gli2 to activate the *Myf5* enhancer to promote myogenesis [60]. At early stages of CGN differentiation, Zic TFs co-localize at many enhancers with the basic helix-loop-helix TF Atoh1. Atoh1 is required for both CGN neurogenesis [30] and differentiation [26] and is highly expressed in CGN progenitors both in rhombic lip of the embryonic hindbrain and in the secondary proliferative zone of the postnatal external granule layer [30, 61]. Unlike the constitutively expressed Zic TFs, *Atoh1* expression turns off when CGNs leave the cell cycle and migrate inward to the internal granule layer. Over the course of CGN differentiation, we observe that Zic binding is lost from about 30% of the sites where it colocalizes with Atoh1 in progenitors (Fig. 2E). Thus, one possible explanation for the transient nature of the early Zic sites is that Atoh1 is required as a co-factor to support Zic binding at these genomic locations. A similar process has been shown to underlie maturation of motor neurons, in which persistently expressed TFs like *Isl1* are handed off between a series of transient enhancers in a manner dependent on the regulated expression of fate-determining TFs like *Lhx3* [62]. In addition to this evidence that Atoh1 may potentially modulate Zic binding, a prior study identified Zic in a one-hybrid screen as a regulatory protein for an enhancer of *Atoh1* that is active during neural tube formation [63]. We demonstrate co-localization of Atoh1 [26] and Zic binding at this *Atoh1* enhancer in early postnatal CGNs (Additional file 1: Fig. S7), further supporting the co-regulatory relationship between these two TFs in early postnatal stages of CGN development. Future studies that determine the effect of manipulating Atoh1 expression on the pattern of Zic binding could experimentally test the function of this relationship.

By contrast, in P60 cerebellum, late Zic TF binding sites are enriched for sequences that can be bound by stimulus-regulated TFs of the Fos, Egr, and MEF2 families. MEF2A/D are well-described regulators of CGN synapse development and granule neuron function in motor learning [51, 64]. Similar to the Zic TFs, not only do MEF2A/D bind sites that contain their canonical sequence specificity, but they also bind to regulatory elements that have AP-1 sequences, which are bound by Fos/Jun family members [64]. Like the Zic TFs, MEF2A and MEF2D are constitutively expressed over the course of CGN differentiation; however, these TFs are subject to stimulus-dependent regulation via post-translational modifications that can switch their functions over time [51]. Phosphorylation of the Zic TFs has been shown to modify their protein-protein interactions in other contexts [22, 44, 60, 65]. Whether phosphorylation of the Zic TFs changes during CGN differentiation and whether post-translational regulation of these factors contributes to differences in their function over time remain open questions.

In addition to sequence-specific DNA binding proteins, we also saw that the Zic TFs colocalize with chromatin regulators. Binding of members of the cohesin complex including CTCF, Rad21, and Smc3 were enriched at the early Zic sites, suggesting Zic TFs could contribute to the function of these complexes in establishing 3D chromatin architecture [66, 67]. The CHARGE syndrome and chromodomain helicase protein *Chd7* is also among the chromatin regulators co-enriched at early Zic TF binding sites. Conditional knockout of *Chd7* in CGN progenitors leads to impairment of accessibility at *Chd7* bound enhancers and results in an unusual pattern of cerebellar gyrification due to changes in the orientation of progenitor division [31]. *Zic2* is known to interact with a different chromodomain helicase, the NuRD complex factor *Chd4*, to maintain pluripotency in embryonic stem cells [44]. Interestingly, conditional knockout of *Chd4* in granule neurons leads to increased accessibility at enhancers as well as increased chromatin interactions at loop boundaries that are normally developmentally repressed [56], highlighting the potential role for chromatin conformation in Zic function [68–70].

Our culture experiments allowed us to define direct, developmentally regulated targets of Zic TFs using a combination of CUT&RUN for Zic binding, RNA-seq in *Zic1/2* knockdown CGNs, and chromatin conformation data. These data provide further support for our hypothesis that Zic TFs function both as transcriptional activators and repressors and they suggest the key biological functions that are regulated by the Zics. Although only a small set of Zic target genes require repression by *Zic1* or *Zic2* for their developmental downregulation,

a substantial number of these genes have functions in neuronal migration and axon guidance. Migration plays an important role in between distinct stages of CGN differentiation. CGN precursors are born in the rhombic lip between E12.5 and E17 in mice [30] and undergo tangential migration across the cerebellar primordium to the external granule layer where they form a secondary proliferative zone [61, 71, 72]. Then, upon cell-cycle exit, newborn CGNs undergo radial migration along the Bergman glia to the internal granule layer [61]. We found that *Zic1/2* are required in cultured CGNs to turn off target genes that are critical for CGN migration (*Barhl1*, *Dcc*, *Epha3*, *ErbB4*, *Nrg3*) [58, 73–79] and axon guidance (*Cntn2*, *Dpys15*, *Nhlh1*, *Tubb2b*, *Robo2*) [26, 31, 57, 72, 80–82]. Interestingly, *Zic2* has previously been suggested to regulate neuronal migration via its function as an activator of *EphB1* and *EphA4* expression in retinal ganglion cells and dorsal spinal cord neurons respectively [83–85], whereas our data show that in CGNs both *Zic1* and *Zic2* function as repressors of a different Ephrin ligand (*Epha3*). The consequence of deleting *Zic* TFs in postmitotic CGNs for cellular positioning has not studied, but our data would predict the *Zic* TFs might be required for the cessation of migration once newborn CGN reach the IGL, which could be studied cell-autonomously [86].

The developmentally regulated genes that are activated by *Zic1/2* binding in postmitotic CGNs are overwhelmingly related to CGN maturation. The gene with the largest number of associated *Zic* binding sites is the transcriptional repressor *Bcl6*. In CGN progenitors, *Bcl6* represses the expression of *Gli* genes to block sonic hedgehog-driven proliferation, which is associated with medulloblastoma [87]. In cortical progenitors, *Bcl6* recruits *Sirt1* to the *Hes5* promoter to drive neuronal differentiation even in the presence of notch signaling, suggesting this repressor has a broad pro-neurogenic function in neural progenitors [88]. A substantial group of *Zic*-dependent developmentally upregulated genes participate in synaptic function (*Gabrd*, *Slc17a7*, *Gprc5b*) and neuronal excitability (*Fgf12*, *Kcnc4*, *Kcnn2*, *Kcnq3*, *Kcnj9*, *Dpp10*), and *Zic* TFs appear to co-regulate groups of genes that coordinate these processes. For example, the candidate *Zic* TF target *Tiam1* is known to activate Rho-GTPase signal cascades to promote synaptic and dendritic plasticity [89–93]. Genes that are upstream regulators of *Tiam1* (*Klf13* and Ephrins) and also those involved in Rho-GTPase signaling (*Rasal1*, *Fgd5*, *Plekhhg1*, *Arhged3*, *Net1*) are also candidate *Zic* targets [94].

While this study provides substantial evidence of targets of *Zic* TFs during CGN development, it is important to note the limitations of these analyses. TF enrichment via BART uses published ChIP-seq data sets acquired from many tissue types and cell lines. Subsequently,

binding of TFs in non-neuronal and non-CGN cell types cannot be directly inferred in this setting. To overcome this limitation, we only searched for enrichment of TFs within *Zic* ChIP peaks which primarily overlapped markers of open chromatin (H3K27ac peaks and DHSs), and for enriched TFs to remain in the analyses, they had to be expressed at respective timepoints. Additionally, though our analyses use a combination of *Zic* binding and CGN gene expression from *Zic1* and *Zic2* KD to determine developmental targets of *Zic*, further studies such as CRISPR deletion of the binding sites followed RT-qPCR of candidate genes would more fully validate these targets. Finally, the antibody used for ChIP recognizes both *Zic1* and *Zic2* but not the other *Zic* family members. Although *Zic1* and *Zic2* are the most highly expressed *Zics* in the cerebellum, there could be roles for *Zic3-5* at some of the *Zic* binding sites studied here.

Conclusions

Using a multi-omics approach, we characterized the genomic features of *Zic* TF binding sites over stages of CGN maturation and investigated the regulatory logic of *Zic* TFs for gene expression during development. We show that different TF families co-bind with the *Zic* TFs at early versus late stages of CGN maturation and suggest that these collaborative factors shape *Zic* TF function. We find that *Zic* TFs are required for both repression and activation of gene expression as neurons mature, though these changes occur largely independent of changes in *Zic* TF binding. Finally, we establish a validated set of direct *Zic* target genes in developing CGNs, which point toward functions of the *Zics* in migration and synaptic function.

Methods

ChIP-seq and DHS data analysis

Zic ChIP-seq, H3K27ac ChIP-seq, and DNase hypersensitivity (DHS) data from postnatal day 7 (P7) and P60 mouse cerebellum were previously generated in [18] and reanalyzed here. ChIP-seq reads were aligned to Gencode GRCm38 vM21 genome using STAR v. 2.7.2b. Duplicate ChIP reads were filtered out and peaks were called using MACS2 v. 2.1.2 with the parameters (–narrow –no-model –ext 147). bedtools2 was used to make a consensus peak set (bedtools intersect merge) and remove (bedtools subtract) the mm10 blacklisted regions [95] for differential analysis. The peak count matrix was generated by estimating the number of reads from the consensus set using RSubreads::featurecounts() v. 2.10.5. These counts were analyzed for differential enrichment between P7 and P60 using default parameters of DESeq2 v 1.36.0 (FDR adjusted *p*-value < 0.05).

Zic1/2 motif analysis

Zic1 and Zic2 motifs were found using Find Individual Motif Occurrences (FIMO) from the MEME-Suite v. 5.3.3 [20].

Identifying potential TFs co-binding at P7 and P60 Zic ChIP peaks

A multi-pronged approach was used to predict TFs that may co-bind with Zic TFs in CGNs. First, we used a PWM-based method (HOMER v. 4.11) [24] to identify TF motifs enriched within Zic ChIP peaks, with the default random GC% matched sequence as background. Second, we used a data driven method (BART v. 2.0) [25, 96] to identify TFs that overlap with *in vivo* Zic ChIP-seq binding. We use these two methods to identify direct binding, via motif enrichment, and possible indirect binding, via enrichment of ChIP binding. In order to focus the analysis on Zic co-factors, enrichment of Zic1 and Zic2 were filtered out.

To statistically compare enriched TFs between P7 and P60 peak sets, a Rank-Rank hyper-geometric overlap test [97] was performed that compared the ranked *p*-value of each enriched TF at P7 to the ranked *p*-value of each enriched TF at P60 separately for the two methods above (BART or HOMER) as a means to calculate significantly concordant TF enrichment (hypergeometric $p < 0.05$). This resulted in identification of a subset of the enriched TFs in each peak set (e.g., P7) that were distinctly enriched in comparison to those from the other peak set (e.g., P60).

The gene expression for each predicted TF whose binding motif or ChIP signal was enriched within the early or late Zic ChIP peaks was calculated using previously published CGN RNA-seq data [18]. To further determine TFs that play timepoint-dependent roles in CGN development, TFs were filtered for normalized mean gene expression > 100 to eliminate poorly expressed genes and for being differential expressed between P7 and P60, which was assessed by DESeq2 (FDR < 0.05 , P7 vs P60).

ChIP overlap analysis

The feature bedtools intersect was used to identify the early, static, and late Zic peaks that intersected with binding of the bHLH TF Atoh1 in CGNs, as determined from a previously published dataset [26]. The percent of overlap was calculated by examining how many Zic ChIP peaks had at least 1 bp overlap with ChIP peaks from the other dataset.

Mapping Zic ChIP peaks to genes via chromatin loops

Zic ChIP-seq peaks were mapped to genes using previously published predicted promoter-enhancer loops derived from adult (P56) cerebellum H3K4me3

PLAC-seq data [54] and juvenile (P22) cerebellum from Hi-C data [55, 56]. ChIP peaks that overlapped the 10 kb anchor bins of these loops using bedtools intersect were considered to be within the promoter-enhancer interactions. The anchors of these loops were annotated to their nearest genes using ChIPSeekR v. 1.32.1 [98]. For each loop, the anchor that was nearest to a gene was deemed the promoter anchor, and the other anchor was deemed the enhancer anchor. The gene mapped to the promoter anchor was assigned to the loop as the target. For cases where both anchors overlapped gene promoters, then both anchors were deemed promoter anchors and both genes were assigned to the loop.

RNA-seq analysis

CGN RNA-seq data were described in a previous study [18] and are reanalyzed here. Raw fastq reads were aligned to the GRCm38 Gencode vM21 genome using STAR v. 2.7.2b. Counts were extracted using HTSeq v. 0.6.1. Normalized bigwigs were made using deepTools bamcoverage v 2.0 (parameters `-effectiveGenomeSize 273,087,177 -ignoreForNormalization chrX`) and visualized using the Gviz R package v 3.15 [99]. Default parameters of DESeq2 v1.36.0 was used to obtain differential expressed genes using an FDR cutoff of 0.05 [100].

CGN cultures and nuclear isolation

CGNs from male and female CD1 mice at P7 were cultured following our published protocols [18]. All procedures were performed under a protocol approved by the Duke University Institutional Animal Care and Use Committee. Briefly, the cerebellum was removed and dissociated with papain, granule neuron progenitors were purified by centrifugation through a Percoll gradient, and neurons were plated on poly-D-lysine coated plates in neurobasal media with B27 supplements, 1% FBS, and pen-strep. At DIV2, cultures were treated with 1 μ M Cytosine Arabinoside (AraC) to block the division of any non-neuronal cells. CGNs at the indicated endpoints were scraped into 1X DPBS, spun down, resuspended in Nuclei Isolation Buffer (20 mM HEPES pH 7.9, 10 mM KCl, 2 mM Spermidine, 0.1% v/v Triton X-100, 20% v/v glycerol), incubated on ice for 5 min, and then spun at 2000 g for 5 min at 4 °C. Pelleted nuclei were resuspended in Nuclei Storage Buffer (20 mM Tris-HCl pH 8.0, 75 mM NaCl, 0.5 mM EDTA, 50% v/v glycerol, 1 mM DTT, 0.1 mM PMSF) at -80 °C until ready to process.

Zic CUT&RUN

CUT&RUN was performed using the CUTANA ChIC/CUT&RUN kit (EpiCypher 14-1408) as per manufacturer guidelines with the specific changes noted here. Nuclei were resuspended in Nuclei Isolation Buffer and

incubated with activated ConA beads. We used an anti-Zic1/2 C-terminal antibody provided courtesy of R. Segal, Harvard Medical School [101], which is the same antibody we used in [18]. CUT&RUN libraries were made using the NEB Ultra II DNA Library Prep Kit for Illumina (NEB E7645L) and NEBNext Multiplex Oligos for Illumina (96 Unique Dual Index Primer Pairs) (NEB E6440S). Library cleanup was performed prior to and after PCR amplification using 0.8X Kapa Hyperpure beads (Roche 08963851001). PCR amplification was performed with the following parameters as described in the EpiCypher CUT&RUN kit: (1) 98 °C, 45 s; (2) 98 °C, 15 s; 60 °C, 10 s × 14 cycles; (3) 72 °C, 60 s. Libraries were then pooled and 50 bp paired-end sequencing was performed at the Duke Sequencing and Analysis Core Resource on a NovaSeq 6000 S-Prime flow cell.

CUT&RUN raw fastq read files were analyzed with FastQC and processed with Trimmomatic 0.38 for quality control and adapter trimming. Trimmed reads were then aligned to the GRCm38 Gencode vM21 reference genome using STAR 2.7.2b. Duplicates were filtered from the resulting alignments with MACS2 2.1.2 filterdup keeping only one duplicate. Genome coverage was calculated using bedtools v2.25.0 genomecov and normalized by sequencing depth. Peak calling was performed with the genome coverage file using SEACR 1.3 stringent with a numeric cutoff that returned the 0.01 fraction of peaks with top signal. A union peak file was obtained with the union function from GenomicRanges 1.48.0 R package. Raw reads were counted using this union peak file as reference with the regionCounts function from the csaw 1.30.1 R package. DESeq2 1.36.0 was used to obtain differentially bound peaks between timepoints, using an adjusted *p* value cutoff of 0.05. Raw counts were used internally by DESeq2 to estimate sample-specific normalization factors that can account for differences in sequencing depth and library composition between samples. Log2 fold change estimates were shrunk using the lfcShrink function from DESeq2, and the ash method.

Identification of direct gene targets of Zic TFs in CGNs

To find genes that are both direct targets of regulation by Zic1/2 and developmentally regulated during CGN differentiation, we integrated (1) genomic Zic binding data in cultured CGNs from Cut&Run-seq with (2) chromatin conformation data to map peaks to genes and (3) changes in the expression of those target genes over developmental time in culture in control or *Zic1/Zic2* knockdown (KD) CGNs [18]. From [18], we obtained ranked lists of gene expression changes across development of CGNs (from 3 to 7 days in vitro (DIV)) in control neurons and changes in gene expression at DIV7 comparing control with either *Zic1* or *Zic2* knockdown. We reanalyzed

these data sets by aligning them to GRCm38 Gencode vM21 genome and performing differential expression analysis with default parameters of DESeq2 1.36.0. We first identify a set of genes that are regulated by Zic, either directly or indirectly by comparing developmentally expressed genes (DIV3 v. DIV7) to differentially expressed genes in *Zic1/2* KD conditions (*ZIC1/2* KD DIV& v WT DIV7) using a Rank-Rank hypergeometric overlap test [102]. Here, we considered genes that were discordantly expressed between the two comparisons as Zic dependent developmental genes. We next identified genes with overlapping Zic CUT&RUN peaks in their respective promoter and enhancer anchors from the P22 chromatin looping data [56] following the methods as described above for the Zic ChIP data and considered these genes to be direct targets of Zic binding. Intersecting the lists of Zic dependent developmental genes and direct Zic target genes resulted in what we called the set of direct Zic regulatory target genes. The R package clusterProfiler v 4.4.1 was used to find enriched Gene Ontology enrichments of Zic target genes, with the background set being all mouse genes.

Abbreviations

BART	Binding Analysis for Regulation of Transcription
BP	Biological Process (reference to gene ontology enrichment)
CGN	Cerebellar granule neuron
ChIP	Chromatin immunoprecipitation
CRISPR	Clustered regularly interspaced short palindromic repeats
DIV	Days in vitro
FC	Fold change
FIMO	Find Individual Motif Occurrences
FDR	False discovery rate
GO	Gene Ontology
HOMER	Hypergeometric Optimization of Motif EnRichment
KD	Knockdown
RRHO	Rank-rank hypergeometric overlap
TF	Transcription factor
ZDD	Zic dependent and developmental regulated

Supplementary Information

The online version contains supplementary material available at <https://doi.org/10.1186/s12915-024-01989-9>.

Additional file 1: Supplementary Figures S1-S7. Fig. S1. Characteristics of Zic Peaks. A) Distribution of the size (bp width) of all Zic ChIP peaks in the union set of all samples at P7 and P60. Consensus sequence of B) *Zic1* and C) *Zic2* motifs searched in the set of all Zic ChIP peaks. D) Distribution of the number of *Zic1* and *Zic2* motifs in early, static, and late Zic ChIP peaks. Fig. S2. In vivo ChIP peak overlap enrichment and motif enrichment of putative co-regulatory TFs in Zic ChIP-seq peaks. Significantly enriched TF motifs from Homer (black) and in vivo ChIP peaks from BART (orange) within A) early or B) late Zic ChIP peaks are shown. TFs that are in both databases used by HOMER and BART are blue and TFs annotated with a * denotes enrichment with both HOMER and BART tools. C) Venn Diagram showing the overlap of the TFs within the BART (orange) and HOMER (black) databases. Heatmap of RRHO *p*-values comparing the D) Motif and E) In vivo ChIP enrichment of TF binding in early and late Zic peaks. Fig. S3. Identification of Zic ChIP peaks that overlap Hi-C anchors. Number of Zic ChIP peaks that overlap P22 (juvenile) cerebellar Hi-C anchors from [56] and P56 (adult) PLAC-seq cerebellar anchors from [54]. Data are sorted by A) the change in gene expression over time (P7 to P60) of the target

gene and B) the change in Zic binding over time of the Zic peaks that overlap the anchors. C) Venn diagram shows the overlap and non-overlap (unique) of anchors from the juvenile (P22, HiC) and adult (P56, PLAC-seq) cerebellum. Fig. S4. The number of Zic peaks that map to a target gene does not determine the direction of gene regulation over developmental time. A) Count of Zic1/2 ChIP-seq peaks mapped to each gene where the color indicates whether the gene is upregulated (red), downregulated (blue) or constitutively expressed (black) from P7 to P60. B) Distribution densities of number of Zic peaks by expression enrichment at different developmental stages. Scatterplots of C) mean expression and D) absolute log fold change of gene expression levels versus the number of Zic peaks. Fig. S5. Zic1/2 CUT&RUN time-course shows dynamic changes in binding during development of cultured CGNs. Zic CUT&RUN was performed in cultured CGNs at 1, 3, 5, and 7 days in vitro (DIV). MA plots comparing Zic peaks called by SEACR showing the differential peaks between A) DIV7 v. DIV1 B) DIV7 v. DIV3 C) DIV7 v. DIV5 E) DIV3 v. DIV1 F) DIV5 v. DIV1 and G) DIV5 v. DIV3. Principal component analysis of Zic in culture and in vivo using the SEACR-called CUT&RUN peaks of G) All in culture samples and H) all in vivo samples. I) Heatmap of Zic CUT&RUN peak intensity for all peaks that are significantly higher at DIV1 or DIV7 from (A). Fig. S6. Comparison of gene expression throughout a developmental time course in cultured cerebellar granule neurons. Volcano plots show the differential genes between A) DIV7 v. DIV3, B) Zic1 KD v. WT at DIV7, and C) Zic2 KD v. WT at DIV7. Heatmap of RRHO *p*-values comparing genes changing throughout WT development versus D) with Zic1 KD and E) with Zic2 KD. Fig. S7: Zic binding at *Atoh1* gene. Tracks of Zic ChIP and Atoh1 ChIP binding at the *Atoh1* gene. Tracks are annotated with early, static, and late Zic ChIP peaks and show early and static Zic peaks near the *Atoh1* gene.

Additional file 2. Differential Zic ChIP-seq Peaks.

Additional file 3. Distinctly enriched transcription factor binding from custom workflow (described in Methods).

Additional file 4. Chromatin Loop, anchor to gene and anchor to Zic peak mapping.

Additional file 5. In-vitro CUT&RUN differential binding, in-vitro RNA-seq differential expression, RRHO enrichment, and GO enrichment terms for candidate Zic targets.

Acknowledgements

We thank Yue Yang (Northwestern) for sharing the predicted mouse cerebellar PLAC-seq loops, Jared Goodman (Washington University, St. Louis) for sharing the predicted mouse cerebellar Hi-C loops, and Irene Kaplow (Carnegie Mellon University) for critical reading of the manuscript.

Code availability

Scripts used for this analysis are deposited at Zenodo. West Lab @ Duke, & Melyssa Minto. (2024). MelyssaMinto/zic_analysis: Release of Genome binding properties of Zic transcription factors underlie their changing functions during neuronal maturation (v1.0.0-main-analysis). Zenodo. <https://doi.org/https://doi.org/10.5281/zenodo.13152077>. (2024).

Authors' contributions

This study was conceived by M.S.M. and A.E.W. Data was gathered by V.R., analyzed by M.S.M. and J.E.S. This manuscript was written by M.S.M. and A.E.W. All authors read, contributed to editing, and approved the final manuscript.

Funding

This work was supported by NIH grant R01-NS098804 (A.E.W.)

Availability of data and materials

All data and code generated or analyzed during this study are included in this published article, its supplementary information files, and/or publicly available repositories.

Mouse cerebellar Zic1/2 ChIP-seq, DNase-seq, Zic1 and Zic2 knockdown RNA-seq, and RNA-seq data from CGNs at DIV3 and DIV7 or cerebellum at P7 and P60 were generated in [18], and the publicly available data can be found at GEO:GSE60731. Frank CL, Liu F, Wijayatunge R, Song L et al. Regulation

of chromatin accessibility and Zic binding at enhancers in the developing cerebellum. GEO datasets. <https://www.ncbi.nlm.nih.gov/geo/query/acc.cgi?acc=GSE60731> (2015).

Atoh1 ChIP-seq data are from [26], and we downloaded the data from GEO: GSE22111.

Klisch TJ, Xi Y, Flora A, Wang L et al. In vivo Atoh1 targetome reveals how a proneural transcription factor regulates cerebellar development. GEO datasets. <https://www.ncbi.nlm.nih.gov/geo/query/acc.cgi?acc=GSE22111> (2011).

Adult PLAC-seq data are from [54], and we downloaded the data from GEO:GSE127995.

Yamada T, Yang Y, Valnegri P, Juric I et al. Sensory experience remodels genome architecture in neural circuit to drive motor learning. GEO datasets. <https://www.ncbi.nlm.nih.gov/geo/query/acc.cgi?acc=GSE127995> (2019).

Juvenile Hi-C data are from [56], and we downloaded the data from GSE138822.

Goodman JV, Yamada T, Yang Y, Kong L et al. The chromatin remodeling enzyme Chd4 regulates genome architecture in the mouse brain. GEO datasets.

<https://www.ncbi.nlm.nih.gov/geo/query/acc.cgi?acc=GSE138822> (2020). Zic1/2 CUT&RUN data were generated in this study and can be found at GSE211309.

Minto, MM, Sotelo-Fonseca, JM, Ramesh, V and West, AE Genome binding properties of Zic transcription factors underlie their changing functions during neuronal maturation. GEO datasets.

<https://www.ncbi.nlm.nih.gov/geo/query/acc.cgi?acc=GSE211309> (2024).

Declarations

Ethics approvals and consent to participate

All animal experiments were performed under protocols A035-20-02 or A025-23-01 (A.E.W.), approved by the Duke University Institutional Animal Care and Use Committee.

Consent for publication

Not applicable.

Competing interests

The authors declare that they have no competing interests.

Received: 6 February 2024 Accepted: 21 August 2024

Published online: 02 September 2024

References

- Hobert O. Regulatory logic of neuronal diversity: terminal selector genes and selector motifs. *Proc Natl Acad Sci U S A*. 2008;105(51):20067–71.
- Telley L, Govindan S, Prados J, Stevant I, Nef S, Dermitzakis E, Dayer A, Jabaudon D. Sequential transcriptional waves direct the differentiation of newborn neurons in the mouse neocortex. *Science*. 2016;351(6280):1443–6.
- Ypsilanti AR, Pattabiraman K, Catta-Preta R, Golonzhka O, Lindtner S, Tang K, Jones IR, Abnousi A, Juric I, Hu M et al. Transcriptional network orchestrating regional patterning of cortical progenitors. *Proc Natl Acad Sci USA*. 2021;118(51):e2024795118.
- Nord AS, West AE. Neurobiological functions of transcriptional enhancers. *Nat Neurosci*. 2020;23(1):5–14.
- Moore JE, Purcaro MJ, Pratt HE, Epstein CB, Shores N, Adrian J, Kawli T, Davis CA, Dobin A, Kaul R, et al. Expanded encyclopaedias of DNA elements in the human and mouse genomes. *Nature*. 2020;583(7818):699–710.
- Aruga J. The role of Zic genes in neural development. *Mol Cell Neurosci*. 2004;26(2):205–21.
- Aruga J, Tohmonda T, Homma S, Mikoshiba K. Zic1 promotes the expansion of dorsal neural progenitors in spinal cord by inhibiting neuronal differentiation. *Dev Biol*. 2002;244(2):329–41.

8. Blank MC, Grinberg I, Aryee E, Laliberte C, Chizhikov VV, Mark Henkelman R, Millen KJ. Multiple developmental programs are altered by loss of *Zic1* and *Zic4* to cause Dandy-Walker malformation cerebellar pathogenesis. *Development*. 2011;138(6):1207–16.
9. Murillo B, Ruiz-Reig N, Herrera M, Fairén A, Herrera E. *Zic2* controls the migration of specific neuronal populations in the developing forebrain. *J Neurosci*. 2015;35(32):11266–80.
10. Merkle FT, Fuentealba LC, Sanders TA, Magno L, Kessarisi N, Alvarez-Buylla A. Adult neural stem cells in distinct microdomains generate previously unknown interneuron types. *Nat Neurosci*. 2014;17(2):207–14.
11. Aruga J. *Zic* family proteins in emerging biomedical studies. *Adv Exp Med Biol*. 2018;1046:233–48.
12. Grinberg I, Northrup H, Ardinger H, Prasad C, Dobyns WB, Millen KJ. Heterozygous deletion of the linked genes *ZIC1* and *ZIC4* is involved in Dandy-Walker malformation. *Nat Genet*. 2004;36(10):1053–5.
13. Brown SA, Warburton D, Brown LY, Yu C-Y, Roeder ER, Stengel-Rutkowski S, Hennekam RCM, Muenke M. Holoprosencephaly due to mutations in *ZIC2*, a homologue of *Drosophila odd-paired*. *Nat Genet*. 1998;20(2):180–3.
14. Gallegos DA, Minto M, Liu F, Hazlett MF, Aryana Yousefzadeh S, Bartelt LC, West AE. Cell-type specific transcriptional adaptations of nucleus accumbens interneurons to amphetamine. *Mol Psychiatry*. 2023;28(8):3414–28.
15. Rudolph T, Yonezawa M, Lein S, Heidrich K, Kubicek S, Schäfer C, Phalke S, Walther M, Schmidt A, Jenuwein T, et al. Heterochromatin formation in *Drosophila* is initiated through active removal of H3K4 methylation by the LSD1 homolog SU (VAR)3–3. *Mol Cell*. 2007;26(1):103–15.
16. Yokota N, Aruga J, Takai S, Yamada K, Hamazaki M, lwase T, Sugimura H, Mikoshiba K. Predominant expression of human *zic* in cerebellar granule cell lineage and medulloblastoma. *Cancer Res*. 1996;56(2):377–83.
17. Gallegos DA, Chan U, Chen LF, West AE. Chromatin regulation of neuronal maturation and plasticity. *Trends Neurosci*. 2018;41(5):311–24.
18. Frank CL, Liu F, Wijayatunge R, Song L, Biegler MT, Yang MG, Vockley CM, Safi A, Gersbach CA, Crawford GE, et al. Regulation of chromatin accessibility and *Zic* binding at enhancers in the developing cerebellum. *Nat Neurosci*. 2015;18(5):647–56.
19. Sepp M, Leiss K, Murat F, Okonechnikov K, Joshi P, Leushkin E, Spanig L, Mbengue N, Schneider C, Schmidt J, et al. Cellular development and evolution of the mammalian cerebellum. *Nature*. 2024;625(7996):788–96.
20. Ma W, Noble WS, Bailey TL. Motif-based analysis of large nucleotide data sets using MEME-ChIP. *Nat Protoc*. 2014;9(6):1428–50.
21. Kulakovskiy IV, Vorontsov IE, Yevshin IS, Sharipov RN, Fedorova AD, Rumynskiy EI, Medvedeva YA, Magana-Mora A, Bajic VB, Papatsenko DA, et al. HOCOMOCO: towards a complete collection of transcription factor binding models for human and mouse via large-scale ChIP-Seq analysis. *Nucleic Acids Res*. 2018;46(D1):D252–d259.
22. Hatayama M, Aruga J. Role of *Zic* family proteins in transcriptional regulation and chromatin remodeling. *Adv Exp Med Biol*. 2018;1046:353–80.
23. Kim T-K, Worley PF, Kuhl D, Kreiman G, Greenberg ME, Bear DM, Harmin DA, Markenscoff-Papadimitriou E, Kuersten S, Gray JM, et al. Widespread transcription at neuronal activity-regulated enhancers. *Nature*. 2010;465(7295):182–7.
24. Heinz S, Benner C, Spann N, Bertolino E, Lin YC, Laslo P, Cheng JX, Murre C, Singh H, Glass CK. Simple combinations of lineage-determining transcription factors prime cis-regulatory elements required for macrophage and B cell identities. *Mol Cell*. 2010;38(4):576–89.
25. Zhenjiawang Z, Civelek M, Miller CL, Sheffield NC, Guertin MJ, Zang C. BART: a transcription factor prediction tool with query gene sets or epigenomic profiles. *Bioinformatics*. 2018;34(16):2867–9.
26. Klisch TJ, Xi Y, Flora A, Wang L, Li W, Zoghbi HY. In vivo Atoh1 targetome reveals how a proneural transcription factor regulates cerebellar development. *Proc Natl Acad Sci USA*. 2011;108(8):3288–93.
27. Aruga J, Hatayama M. Comparative Genomics of the *Zic* Family Genes. *Adv Exp Med Biol*. 2018;1046:3–26.
28. Yeung J, Ha TJ, Swanson DJ, Choi K, Goldowitz D, Tong Y. Wls provides a new compartmental view of the rhombic lip in mouse cerebellar development. *J Neurosci*. 2014;34(37):12527–37.
29. Wang VY, Rose MF, Zoghbi HY. *Math1* expression redefines the rhombic lip derivatives and reveals novel lineages within the brainstem and cerebellum. *Neuron*. 2005;48(1):31–43.
30. Ben-Arie N, Bellen HJ, Armstrong DL, McCall AE, Gordadze PR, Guo Q, Matzuk MM, Zoghbi HY. *Math1* is essential for genesis of cerebellar granule neurons. *Nature*. 1997;390(6656):169–72.
31. Reddy NC, Majidi SP, Kong L, Nemer M, Ferguson CJ, Moore M, Goncalves TM, Liu HK, Fitzpatrick JAJ, Zhao G, et al. CHARGE syndrome protein CHD7 regulates epigenomic activation of enhancers in granule cell precursors and gyrification of the cerebellum. *Nat Commun*. 2021;12(1):1–17.
32. Medina-Martinez O, Haller M, Rosenfeld JA, O'Neill MA, Lamb DJ, Jamrich M. The transcription factor *Maz* is essential for normal eye development. *Dis Model Mech*. 2020;13(8):dmm044412.
33. Song J, Xie C, Jiang L, Wu G, Zhu J, Zhang S, Tang M, Song L, Li J. Transcription factor AP-4 promotes tumorigenic capability and activates the Wnt/ β -catenin pathway in hepatocellular carcinoma. *Theranostics*. 2018;8(13):3571–83.
34. Hsu YC, Kao CY, Chung YF, Chen MS, Chiu IM. Ciliogenic RFX transcription factors regulate FGF1 gene promoter. *J Cell Biochem*. 2012;113(7):2511–22.
35. Shy BR, Wu CI, Khramtsova GF, Zhang JY, Olopade OI, Goss KH, Merrill BJ. Regulation of Tcf711 DNA binding and protein stability as principal mechanisms of Wnt/ β -catenin signaling. *Cell Rep*. 2013;4(1):1–9.
36. Liu L, Li Q, Yang L, Li Q, Du X. SMAD4 feedback activates the canonical TGF- β family signaling pathways. *Int J Mol Sci*. 2021;22(18):10024.
37. Nickel J, Mueller TD. Specification of BMP signaling. *Cells*. 2019;8(12):1579.
38. Derynck R, Zhang YE. Smad-dependent and Smad-independent pathways in TGF- β family signalling. *Nature*. 2003;425(6958):577–84.
39. Holz A, Kollmus H, Ryge J, Niederkofler V, Dias J, Ericson J, Stoeckli ET, Kiehn O, Arnold H-H. The transcription factors *Nkx2.2* and *Nkx2.9* play a novel role in floor plate development and commissural axon guidance. *Development*. 2010;137(24):4249–60.
40. Phillips JE, Corces VG. CTCF: master weaver of the genome. *Cell*. 2009;137(7):1194–211.
41. Aranda S, Mas G, Di Croce L. Regulation of gene transcription by polycomb proteins. *Sci Adv*. 2015;1(11):e1500737.
42. van Wijnen AJ, Bagheri L, Badreldin AA, Larson AN, Dudakovic A, Thaler R, Paradise CR, Wu Z. Biological functions of chromobox (CBX) proteins in stem cell self-renewal, lineage-commitment, cancer and development. *Bone*. 2021;143:115659–115659.
43. Schultz DC, Ayyanathan K, Negorev D, Maul GG, Rauscher FJ. SETDB1: a novel KAP-1-associated histone H3, lysine 9-specific methyltransferase that contributes to HP1-mediated silencing of euchromatic genes by KRAB zinc-finger proteins. *Genes Dev*. 2002;16(8):919–32.
44. Luo Z, Gao X, Lin C, Smith ER, Marshall SA, Swanson SK, Florens L, Washburn MP, Shilatifard A. *Zic2* is an enhancer-binding factor required for embryonic stem cell specification. *Mol Cell*. 2015;57(4):685–94.
45. Schultz DC, Friedman JR, Rauscher FJ. Targeting histone deacetylase complexes via KRAB-zinc finger proteins: the PHD and bromodomains of KAP-1 form a cooperative unit that recruits a novel isoform of the Mi-2 α subunit of NuRD. *Genes Dev*. 2001;15(4):428–43.
46. Abrajano JJ, Qureshi IA, Gokhan S, Zheng D, Bergman A, Mehler MF. REST and CoREST modulate neuronal subtype specification, maturation and maintenance. *PLoS One*. 2009;4(12):e7936.
47. Wu JI, Lessard J, Olave IA, Qiu Z, Ghosh A, Graef IA, Crabtree GR. Regulation of dendritic development by neuron-specific chromatin remodeling complexes. *Neuron*. 2007;56(1):94–108.
48. Janesick A, Wu SC, Blumberg B. Retinoic acid signaling and neuronal differentiation. *Cell Mol Life Sci*. 2015;72(8):1559–76.
49. Kullmann JA, Trivedi N, Howell D, Laumonerie C, Nguyen V, Banerjee SS, Stably DR, Shirinifard A, Rowitch DH, Solecki DJ. Oxygen tension and the VHL-Hif1 α pathway determine onset of neuronal polarization and cerebellar germinal zone exit. *Neuron*. 2020;106(4):607–623.e605.
50. Vierbuchen T, Ling E, Cowley CJ, Couch CH, Wang X, Harmin DA, Roberts CWM, Greenberg ME. AP-1 transcription factors and the BAF complex mediate signal-dependent enhancer selection. *Mol Cell*. 2017;68(6):1067–1082.e1012.
51. Shalizi A, Gaudillière B, Yuan Z, Stegmüller J, Shirogane T, Ge Q, Tan Y, Schulman B, Harper JW, Bonni A. A calcium-regulated MEF2

- sumoylation switch controls postsynaptic differentiation. *Science*. 2006;311(5763):1012–7.
52. West AE, Greenberg ME. Neuronal activity-regulated gene transcription in synapse development and cognitive function. *Cold Spring Harb Perspect Biol*. 2011;3(6):a005744.
 53. Panigrahi A, O'Malley BW. Mechanisms of enhancer action: the known and the unknown. *Genome Biol*. 2021;22(1):108.
 54. Yamada T, Yang Y, Valnegri P, Juric I, Abnoui A, Markwalter KH, Guthrie AN, Godec A, Oldenborg A, Hu M, et al. Sensory experience remodels genome architecture in neural circuit to drive motor learning. *Nature*. 2019;569:708–13 Nature Publishing Group.
 55. Goodman JV, Bonni A. Regulation of neuronal connectivity in the mammalian brain by chromatin remodeling. *Curr Opin Neurobiol*. 2019;59:59–68.
 56. Goodman JV, Yamada T, Yang Y, Kong L, Wu DY, Zhao G, Gabel HW, Bonni A. The chromatin remodeling enzyme Chd4 regulates genome architecture in the mouse brain. *Nat Commun*. 2020;11:1–14.
 57. Jeanne M, Demory H, Moutal A, Vuillaume M-L, Blesson S, Thépault R-A, Marouillat S, Halewa J, Maas SM, Motazacker MM, et al. Missense variants in DPYSL5 cause a neurodevelopmental disorder with corpus callosum agenesis and cerebellar abnormalities. *Am J Hum Genet*. 2021;108(5):951–61.
 58. Shi M, Guo C, Dai J, Ding Y. DCC is required for the tangential migration of noradrenergic neurons in locus coeruleus of mouse brain. *Mol Cell Neurosci*. 2008;39(4):529.
 59. Breuss MW, Leca I, Gstrein T, Hansen AH, Keays DA. Tubulins and brain development - the origins of functional specification. *Mol Cell Neurosci*. 2017;84:58–67.
 60. Himeda CL, Barro MV, Emerson CP. Pax3 synergizes with Gli2 and Zic1 in transactivating the Myf5 epaxial somite enhancer. *Dev Biol*. 2013;383(1):7–14.
 61. Rahimi-Balaei M, Bergen H, Kong J, Marzban H. Neuronal migration during development of the cerebellum. *Front Cell Neurosci*. 2018;12:484.
 62. Rhee HS, Closser M, Guo Y, Bashkirova EV, Tan GC, Gifford DK, Wichterle H. Expression of terminal effector genes in mammalian neurons is maintained by a dynamic relay of transient enhancers. *Neuron*. 2016;92(6):1252–65.
 63. Ebert PJ, Timmer JR, Nakada Y, Helms AW, Parab PB, Liu Y, Hunsaker TL, Johnson JE. Zic1 represses Math1 expression via interactions with the Math1 enhancer and modulation of Math1 autoregulation. *Development*. 2003;130(9):1949–59.
 64. Majidi SP, Reddy NC, Moore MJ, Chen H, Yamada T, Andzelm MM, Cherry TJ, Hu LS, Greenberg ME, Bonni A. Chromatin environment and cellular context specify compensatory activity of paralogous MEF2 transcription factors. *Cell Rep*. 2019;29(7):2001–2015.e2005.
 65. Ishiguro A, Ideta M, Mikoshiba K, Chen DJ, Aruga J. ZIC2-dependent transcriptional regulation is mediated by DNA-dependent protein kinase, poly(ADP-ribose) polymerase, and RNA helicase A. *J Biol Chem*. 2007;282(13):9983–95.
 66. Zheng H, Xie W. The role of 3D genome organization in development and cell differentiation. *Nat Rev Mol Cell Biol*. 2019;20(9):535–50.
 67. Bonev B, Cavalli G. Organization and function of the 3D genome. *Nat Rev Genet*. 2016;17(11):661–78.
 68. Hamley JC, Li H, Denny N, Downes D, Davies JOJ. Determining chromatin architecture with Micro Capture-C. *Nat Protoc*. 2023;18(6):1687–711.
 69. Kempfer R, Pombo A. Methods for mapping 3D chromosome architecture. *Nat Rev Genet*. 2020;21(4):207–26.
 70. Wei X, Xiang Y, Peters DT, Marius C, Sun T, Shan R, Ou J, Lin X, Yue F, Li W, et al. HiCAR is a robust and sensitive method to analyze open-chromatin-associated genome organization. *Mol Cell*. 2022;82(6):1225–1238. e1226.
 71. Choi Y. Migration from a mitogenic niche promotes cell-cycle exit. *J Neurosci*. 2005;25(45):10437–45.
 72. Chédotal A. Should I stay or should I go? Becoming a granule cell. *Trends Neurosci*. 2010;33(4):163.
 73. Dong H, Yauk C, Wade M. Barhl1 is directly regulated by thyroid hormone in the developing cerebellum of mice. *Biochem Biophys Res Commun*. 2011;415(1):157.
 74. Lopes C, Delezoide A, Delabar J, Rachidi M. BARHL1 homeogene, the human ortholog of the mouse Barhl1 involved in cerebellum development, shows regional and cellular specificities in restricted domains of developing human central nervous system. *Biochem Biophys Res Commun*. 2006;339(1):296.
 75. Li S. Barhl1 regulates migration and survival of cerebellar granule cells by controlling expression of the neurotrophin-3 gene. *J Neurosci*. 2004;24(12):3104–14.
 76. Cotrufo T, Andrés R, Ros O, Pérez-Brangulí F, Muhaisen A, Fuschini G, Martínez R, Pascual M, Comella J, Soriano E. Syntaxin 1 is required for DCC/Netrin-1-dependent chemoattraction of migrating neurons from the lower rhombic lip. *Eur J Neurosci*. 2012;36(9):3152.
 77. Karam SD, Burrows RC, Logan C, Koblar S, Pasquale EB, Bothwell M. Eph receptors and ephrins in the developing chick cerebellum: relationship to sagittal patterning and granule cell migration. *J Neurosci*. 2000;20(17):6488–500.
 78. Rio C, Rieff HI, Qi P, Corfas G. Neuregulin and erbB receptors play a critical role in neuronal migration. *Neuron*. 1997;19(1):39–50.
 79. Chen Y, Fu A, Ip N. Bidirectional signaling of ErbB and Eph receptors at synapses. *Neuron Glia Biol*. 2008;4(3):211.
 80. Wang W, Karagogeos D, Kilpatrick DL. The effects of Tag-1 on the maturation of mouse cerebellar granule neurons. *Cell Mol Neurobiol*. 2011;31(3):351–6.
 81. Yamada T, Yang Y, Hemberg M, Yoshida T, Cho HY, Murphy JP, Fioravante D, Regehr WG, Gygi SP, Georgopoulos K, et al. Promoter decommissioning by the NuRD chromatin remodeling complex triggers synaptic connectivity in the mammalian brain. *Neuron*. 2014;83(1):122–34.
 82. Valnegri P, Puram SV, Bonni A. Regulation of dendrite morphogenesis by extrinsic cues. *Trends Neurosci*. 2015;38(7):439–47.
 83. García-Frigola C, Carreres MI, Vegar C, Mason C, Herrera E. Zic2 promotes axonal divergence at the optic chiasm midline by EphB1-dependent and -independent mechanisms. *Development*. 2008;135(10):1833–41.
 84. Escalante A, Murillo B, Morenilla-Palao C, Klar A, Herrera E. Zic2-dependent axon midline avoidance controls the formation of major ipsilateral tracts in the CNS. *Neuron*. 2013;80(6):1392–406.
 85. Herrera E. Rodent Zic genes in neural network wiring. *Adv Exp Med Biol*. 2018;1046:209–30.
 86. Chan U, Gautam D, West AE. Utilizing in vivo postnatal electroporation to study cerebellar granule neuron morphology and synapse development. *J Vis Exp*. 2021;(172):10.3791/62568.
 87. Tiberi L, Bonnefont J, Van den Aemele J, Le Bon SD, Herpoel A, Bilheu A, Baron BW, Vanderhaeghen P. A BCL6/BCOR/SIRT1 complex triggers neurogenesis and suppresses medulloblastoma by repressing sonic hedgehog signaling. *Cancer Cell*. 2014;26(6):797–812.
 88. Tiberi L, van den Aemele J, Dimidschstein J, Piccirilli J, Gall D, Herpoel A, Bilheu A, Bonnefont J, Iacovino M, Kyba M, et al. BCL6 controls neurogenesis through Sirt1-dependent epigenetic repression of selective Notch targets. *Nat Neurosci*. 2012;15(12):1627–35.
 89. Rao S, Kay Y, Herring BE. Tiam1 is critical for glutamatergic synapse structure and function in the hippocampus. *J Neurosci*. 2019;39(47):9306–15.
 90. Cheng J, Scala F, Blanco FA, Niu S, Firozi K, Keehan L, Mulherkar S, Froudarakis E, Li L, Duman JG, et al. The Rac-GEF Tiam1 promotes dendrite and synapse stabilization of dentate granule cells and restricts hippocampal-dependent memory functions. *J Neurosci*. 2021;41(6):1191–206.
 91. Abe H, Okazawa M, Nakanishi S. Gene regulation via excitation and BDNF is mediated by induction and phosphorylation of the ETV1 transcription factor in cerebellar granule cells. *Proc Natl Acad Sci*. 2012;109(22):8734–9.
 92. Wijayatunge R, Liu F, Shpargel KB, Wayne NJ, Chan U, Boua J-V, Magnuson T, West AE. The histone demethylase Kdm6b regulates a mature gene expression program in differentiating cerebellar granule neurons. *Mol Cell Neurosci*. 2018;87:4–17.
 93. Duman JG, Blanco FA, Cronkite CA, Ru Q, Erikson KC, Mulherkar S, Saifullah AB, Firozi K, Tolias KF. Rac-maninoff and Rho-vel: the symphony of Rho-GTPase signaling at excitatory synapses. *Small GTPases*. 2022;13(1):14–47.
 94. Ávila-Mendoza J, Subramani A, Denver R. Krüppel-like factors 9 and 13 block axon growth by transcriptional repression of key components of the cAMP signaling pathway. *Front Mol Neurosci*. 2020;13:602638.

95. Amemiya HM, Kundaje A, Boyle AP. The ENCODE blacklist: identification of problematic regions of the genome. *Sci Rep.* 2019;9(1):9354.
96. Ma W, Wang Z, Zhang Y, Magee NE, Feng Y, Shi R, Chen Y, Zang C. BARTweb: a web server for transcriptional regulator association analysis. *NAR Genom Bioinform.* 2021;3(2):lqab022.
97. Plaisier SB, Taschereau R, Wong JA, Graeber TG. Rank-rank hypergeometric overlap: identification of statistically significant overlap between gene-expression signatures. *Nucleic Acids Res.* 2010;38(17):e169.
98. Yu G, Wang L, He Q. ChIPseeker: an R/Bioconductor package for ChIP peak annotation, comparison and visualization. *Bioinformatics.* 2015;31(14):2382.
99. Hahne F, Ivanek R. Visualizing genomic data using Gviz and bioconductor. *Methods Mol Biol.* 2016;1418:335–51 Springer New York.
100. Love MI, Huber W, Anders S. Moderated estimation of fold change and dispersion for RNA-seq data with DESeq2. *Genome Biol.* 2014;15(12):550.
101. Borghesani PR, Peyrin JM, Klein R, Rubin J, Carter AR, Schwartz PM, Luster A, Corfas G, Segal RA. BDNF stimulates migration of cerebellar granule cells. *Development.* 2002;129(6):1435–42.
102. Cahill KM, Huo Z, Tseng GC, Logan RW, Seney ML. Improved identification of concordant and discordant gene expression signatures using an updated rank-rank hypergeometric overlap approach. *Sci Rep.* 2018;8(1):9588.

Publisher's Note

Springer Nature remains neutral with regard to jurisdictional claims in published maps and institutional affiliations.